Soil Dynamics and Earthquake Engineering 123 (2019) 381–398

Contents lists available at ScienceDirect

Soil Dynamics and Earthquake Engineering

journal homepage: www.elsevier.com/locate/soildyn

Local site effect incorporation in probabilistic seismic hazard analysis – A case study from southern peninsular India, an intraplate region

C. Shreyasvi[a,*], Katta Venkataramana[a], Sumer Chopra[b]

[a] Department of Civil Engineering, National Institute of Technology Karnataka, Surathkal, Mangalore, 575025, India
[b] Institute of Seismological Research, Raysan Road, Gandhinagar, Gujarat, 382009, India

ARTICLE INFO

Keywords:
Nonlinear site amplification
Host to target adjustment
Spectral matching
Site response analysis
North Kerala

ABSTRACT

The inclusion of local site effects into seismic hazard analysis is an important issue and has been attempted previously in both deterministic and probabilistic manner. The present study is an attempt to combine the local site response with the standard probabilistic seismic hazard analysis. The site response was computed by performing an equivalent linear analysis in the frequency domain. The input soil profiles for the analysis were taken from the borehole data of the North Kerala region (one of the Southerly states in India). The uncertainty in estimating the shear velocity profile (V_S) has been addressed by applying multiple V_S–N correlations. The variability in the choice of input motions has been reduced by selecting multiple ground motions representing distinct hazard levels (return period of 50–2000 years). The uniform hazard spectrum developed for the host reference site conditions has been adjusted to the target region and the input motions are scaled accordingly. The analyzed soil profiles were categorized into three distinct soil types namely 'Sand', 'Clay' and 'All soil' based on the predominant soil content. The empirical amplification equation as a function of input rock spectral acceleration (S_a^r) was developed for each soil type. 'Sand' exhibits nonlinear behavior for $S_a^r > 0.1$ g whereas 'clay' demonstrates sustained amplification at longer periods. The average spectral amplification observed is 3 for 'All soil', 5 for 'clay' and 3.5 for 'sand' in the study region. The regionally developed amplification function aids in transforming a Ground Motion Prediction Equation (GMPE) from generic to site-specific. The modified GMPE is integrated with the regional seismic source model to estimate site-specific probabilistic seismic hazard. The study produces site-specific spectrum and surface hazard maps which can be of direct use to planners and designers in creating a seismic resilient built environment.

1. Introduction

A seismic wave propagating from its source towards the surface alters itself in terms of amplitude and direction, consistent with the dynamic characteristics of the medium. This phenomenon is termed as local site – effect and is a collective effort of ground response, basin effects, and topographic effects. The ground response captures impedance, soil nonlinearity and resonance effects of the sediment layers. The local topographic effect causes scattering, focusing, and defocusing of the incident waves. The basin effect has the potential to trap the body waves and generate surface waves of stronger shaking and longer duration.

The influence of local site effects is captured by the dynamic simulation of wave propagation through a series of soil layers (with distinct geotechnical characteristics) laid parallel to each other as shown in Fig. 1. This technique is referred to as site response analysis and various approaches are available to perform the analysis. The site response can be captured in 1D, 2D or 3D, considering linear, equivalent linear or nonlinear soil characteristics using total or effective stress principle. The present study considers 1- D shear wave propagation to model soil nonlinearity represented by an equivalent linear (EQL) approach using effective stress principle.

Any seismic hazard analysis without the inclusion of local site effects is incomplete as the ground motion at the surface is governed by the underlying soil characteristics. The probabilistic seismic hazard analysis (PSHA) estimates the values of ground motion parameters (PGA, PSA, S_a (T)) for a given probability of exceedance (POE) in a chosen time frame. Usually, the hazard values are predicted for a reference rock site condition analogous with the ground motion prediction equation (GMPE) used in PSHA. The surface site condition differs significantly from the reference site condition, hence, a site-specific hazard analysis must include steps to represent the local surface site condition.

* Corresponding author.
E-mail addresses: shreyasvic@gmail.com (C. Shreyasvi), ven.nitk@gmail.com (K. Venkataramana), sumer.isr@yahoo.com (S. Chopra).

https://doi.org/10.1016/j.soildyn.2019.04.035
Received 17 December 2018; Received in revised form 1 March 2019; Accepted 29 April 2019

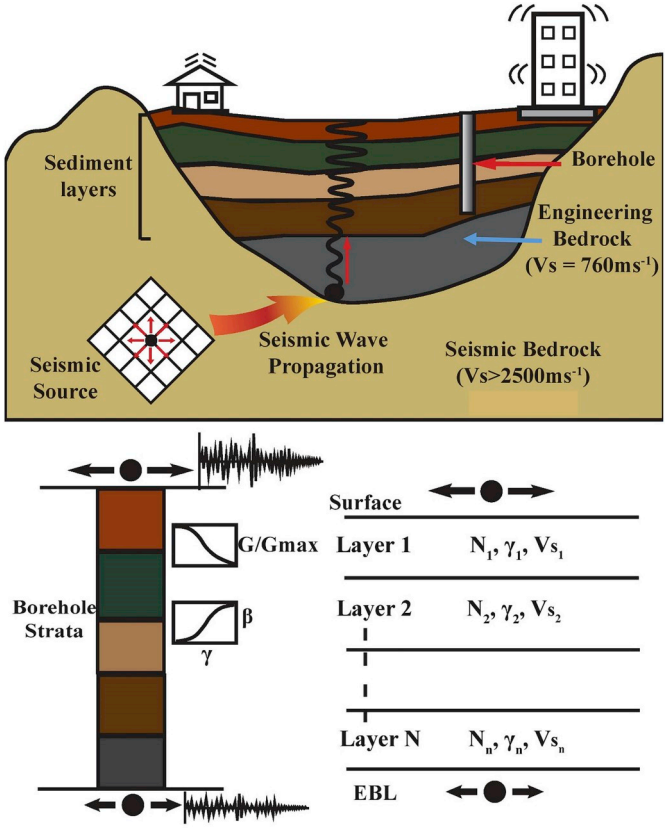

Fig. 1. Illustration of Seismic wave propagation and site response analysis (N - SPT value; γ - unit weight and V_S - shear velocity of 'n' individual strata).

The local site effects are first realized in the form of amplification factor or frequency dependent amplification function and then integrated with PSHA. Various methods with varying levels of complexity are available in making PSHA more and more site-specific. The simplest procedure involves multiplying a rock acceleration response spectrum (from PSHA) with an amplification factor derived for standard soil types. The resulting response spectrum varies in spectral shape depending on the soil type. The Indian seismic code [1] provides a design acceleration coefficient for three standard site conditions namely, soft soil, stiff soil, and hard soil. However, these procedures are deterministic resulting in a response spectrum of unknown POE and are ineffective in site-specific applications.

A probabilistic yet simplistic procedure involves the use of GMPEs with site coefficients defined for different site classes categorized based on $Vs_{(30)}$ (for example [2,3]). However, this approach is considered as ergodic as the site coefficients are derived based on the global databases and may not accurately represent the regional seismic hazard. Hybrid method has been practiced widely which involves simple multiplication of the rock hazard curve of given POE with the mean site amplification. This method is termed as hybrid as it combines a probabilistic rock motion with a deterministic amplification [4]. The standard deviation of the resulting surface level hazard captures the variability in estimating the rock level hazard but fails to account for variability in seismic site amplification. Hence, the procedure is convenient for estimating median surface responses but not the standard deviation. A completely probabilistic procedure involves convolution of rock PSHA with the frequency dependent nonlinear site amplification function [5]. This method supersedes hybrid method as it accounts for uncertainty in site response as well.

The present study investigates the influence of local soil response on the already computed rock level PSHA for the Southwestern region of India. Numerous soil profiles were collected for the study region and 1D EQL was performed on SHAKE2000 [6] to obtain frequency dependent empirical site amplification function for three different soil types such as Sand, Clay, and all soil. The derived amplification function is integrated into PSHA by transforming the rock GMPE into a site-specific one [5]. The seismic hazard values are estimated at the surface level for a known probability of exceedance. The study highlights the inadequacy of $Vs_{(30)}$ as the sole predictor variable for estimating site amplification. The derived surface response spectrum can be used in the analysis and design of earthquake resilient infrastructure for the study region.

2. Description of the study area

The study area encompasses the Northern part of Kerala (one of the southern states in India) stretching between 10.08°N and 12.72°N (latitude) and 74.86°E to 76.85°E (longitude). There are a total of 14 districts in the state out of which 7 districts namely, Kasargod, Kannur, Kozhikode (Calicut), Wayanad, Malappuram, Palakkad, and Ernakulam were chosen for the study as shown in Fig. 2a. Earlier seismic hazard study in the region [7] considered the observed regional seismicity and estimated the ground motion parameter (PGA) at the bedrock level and hence, served as an ideal site to understand local soil amplification. The physiography of the study region can be classified as lowland, midland, and highland as shown in Fig. 2c. The low land comprises of the area adjacent to the coastal stretch whereas the highland encompasses the eastern part of the state consisting of hill stations and a portion of Western Ghats. Midland lies between these two major physiographic divisions characterized by undulating topography gradually transitioning from plain lands to valleys and towards hills. The region slopes towards the west and the elevation vary from 1 m to 2612 m above the mean sea level.

The local terrain is geologically characterized by Pre-Cambrian and Pleistocene formations comprising of granulite, gneisses, granites, and greenstones. Charnockites and charnockitic gneisses occupy the major portion of midland and WesternGhats in North and Central Kerala. One of the characteristic geological features is that the granulitic gneisses are spatially well connected with the regional faults and lineaments [8]. The study area belongs to Southern Granulite Terrain, housing few active tectonic features such as Bhavani Shear, Moyar shear, Cauvery fault, and Pattikad – Kollengal fault. These features are believed to be releasing the stresses accumulated due to the northward movement of the Indian Shield [9] and as an evidence majority of the earthquakes occurring in North Kerala have their epicenters concentrated in and around these tectonic features. The region has witnessed earthquakes with magnitude (M_w) as low as 1.1 and as high as 6.3 and is characterized as moderately seismically active with more than 330 seismic events being recorded over the last few decades. Most of the seismic activity was witnessed over Moyar and Bhavani Shear zones along with few other closely located faults as shown in Fig. 2b. These shear zones are suspected to be releasing the stress accumulated due to the Northward movement of the Indian plate towards the Eurasian plate. The Idukki earthquake (1988) recorded 67 aftershocks and the resulting focal mechanism suggests a strike-slip movement [10].

The topography, climate, and local geology have influenced the local soil formation. Laterite is the most prominent soil type in the study region formed due to weathering of rocks and serves as an excellent building material. This type of soil is observed in heavy rainfall region with humid tropical conditions and rich in iron and aluminum oxides. The surface soils appear in reddish brown to yellowish red in color with a texture varying from gravelly loam to gravelly clay loam. Apart from laterites, the study region is geotechnically characterized by coastal alluvium developed from recent marine deposits and fluvial sediment along the coastal stretch. This soil type is predominantly 'sand' with smaller quantities of silt and clay. In general, the soil deposits observed in Palakkad and Thrissur are deep and well drained with fairly high gravel content and loamy to 'clay' texture. Hence, the collected

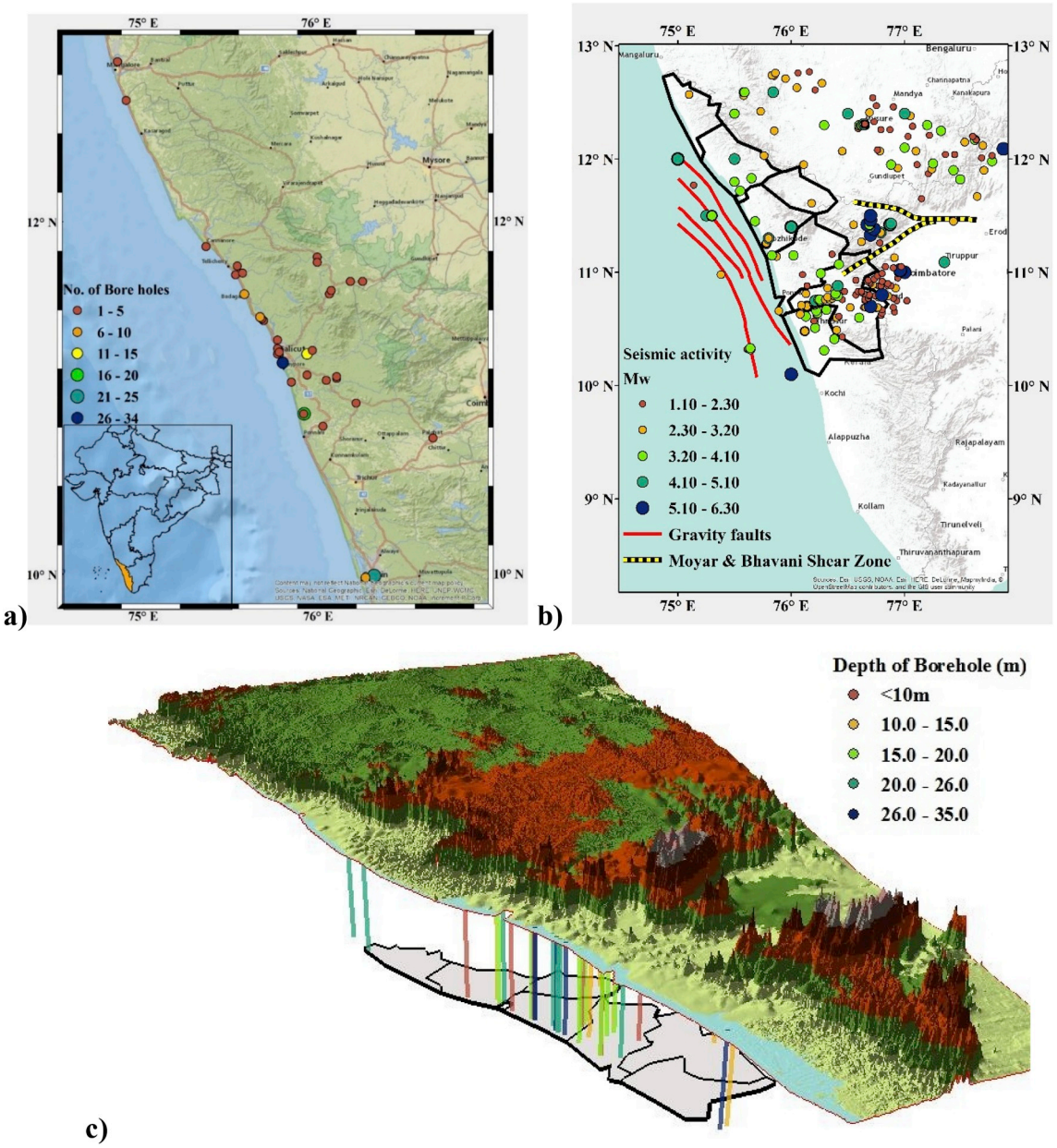

Fig. 2. a) Physical map representing the study area and the number of boreholes used for the study (left) b) Regional seismicity map of the study area (right) c) Topographical map of South Western India with the study area being drop shadowed (Bottom). The boreholes are exaggerated vertically for projecting their geographical locations on the map and the depth of the boreholes are color-coded as indicated in the legend. (For interpretation of the references to color in this figure legend, the reader is referred to the Web version of this article.)

borehole samples consisted of 'sand' deposits close to the coastal tract and 'clay' deposits as well as a mixture of laterites, sand, and clay in the rest of the study region.

The study region has exposures of gneissic rocks close to the beaches and a few other places. The typical geological strata for the Calicut region in the order of their appearance from the ground surface is Sand, Clayey Sand, Clay, laterite, lateritic clay, weathered rock, hard basement rock (gneiss), fractured rock and hard rock [11]. The depth to bedrock varied from 20 m to 35 m depending on the topography [12]. Most of the boreholes were terminated upon reaching the hard rock strata. In places such as Ernakulam and Palakkad, the weathered geological units were observed between 2 and 16 m. In such cases, the validation for the depth to bedrock was derived by referring to the electrical resistivity surveys carried out in the region [13]. However, in Malapurram the depth to compact bedrock is in the range of 50–200 m [14]. In Kannur, the depth to weathered rock ranges between 3 and 20 m. Based on vast literature survey ([15–19], and [20]) and the collected borehole data, it can be concluded that the overall depth to Engineering Bedrock ($V_{S(30)} > 760\ ms^{-1}$) is within 50 m from the surface and the same has been applied for soil profiling in the study.

3. Soil modeling

The soil characteristics form an integral part in modeling the soil profile for seismic site amplification studies. In this regard, the subsurface geology and geotechnics were studied using borehole data determined as per the guidelines of IS 2131 (1981) [21]. The geotechnical data consisting of bore logs with standard penetration test 'N' value, unit weight, index properties, grain size distribution, and shear strength parameters were collected from the Dept. of Civil Engineering, National Institute of Technology Calicut. Additionally, reports of electrical resistivity studies and groundwater information booklets by Central

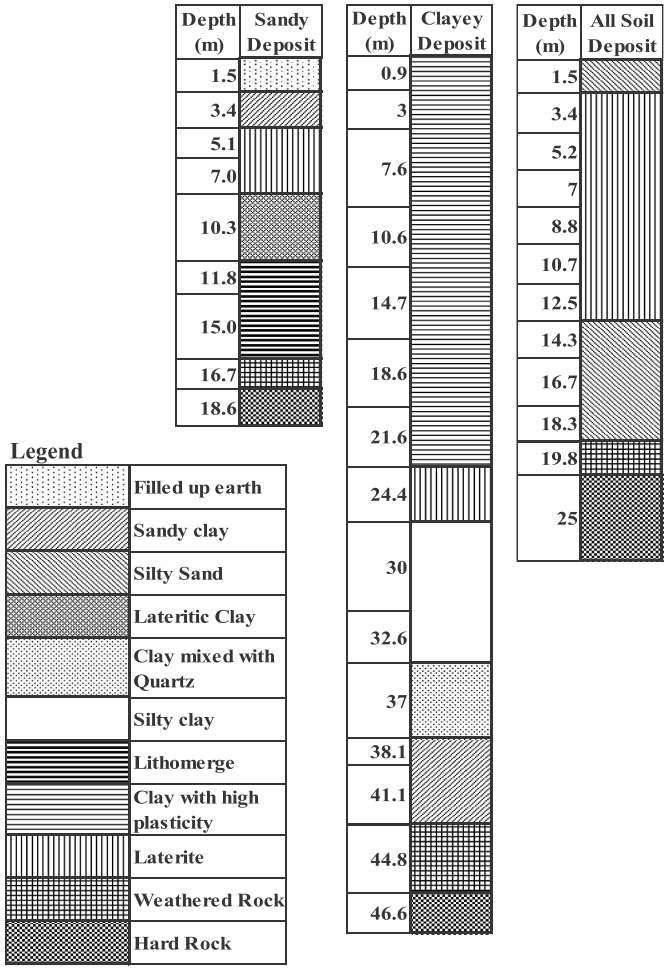

Fig. 3. Stratigraphy of all the three representative soil types used in the study.

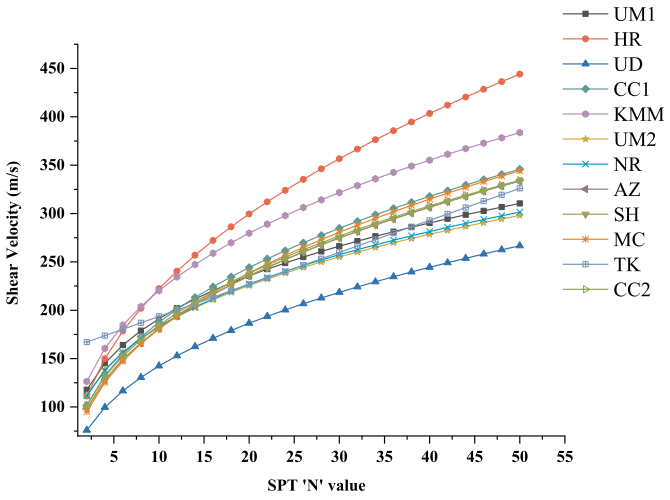

Fig. 4. Comparison of the Vs – N correlations investigated in the study.

Ground Water Board, Govt. of India were referred to understand the subsurface geological and geotechnical formations. The geographical location, depth, and the number of boreholes compiled for the study can be inferred from Fig. 2a and c. The borehole information was collected from approximately 40 locations in the study area with a minimum of two boreholes and a maximum of 30 boreholes at each location. However, on processing the collected data, few borehole samples were discarded due to missing data on *N*-value, unit weight or grain size distribution. The compiled borehole data was classified into three soil types i.e Sand, Clay and All soil based on the predominant soil content and grain size distribution. Overall 30 samples for 'all soil', 15 samples for 'clay' and 6 samples for 'sand' were considered for further analysis. A typical stratigraphy witnessed in a sample borehole of each soil type is shown in Fig. 3. The shear velocity (Vs) profile for all the boreholes was estimated using V_S–N correlation. In order to reduce the uncertainty involved in the estimation of Vs, multiple correlations were investigated as shown in Fig. 4. The details about each of these correlations have been tabulated in Table 1. Importance to regionally developed correlations and based on uncorrected SPT 'N' values was given during the selection process in order to maintain homogeneity. As evident from Fig. 4, few correlations resulted in extreme estimations such as HR, KMM, and UD. These correlations were eliminated and a total of six correlations were used for the final estimation of shear velocity profile. The estimated shear velocity profile from all the six correlations along with the median and standard deviation is shown in Fig. 5.

Apart from estimating the shear velocity for each layer in a soil column, the dynamic characteristics such as normalized shear modulus reduction (G/G_{max}) and damping (D) of these soil layers need to be defined. Various laboratory tests such as Cyclic tri-axial shear or resonant column shear apparatus can be used to estimate the dynamic properties. However, in the absence of experimental programs, empirical relations of G/G_{max} and D as a function of cyclic shear strain (γ_c) can be used as a dynamic soil response curve. These curves are referred to as backbone curves and are developed to capture the nonlinear hysteretic behavior of various soil types. The *M*-R and damping curves chosen for various soil strata are tabulated in Tables 2–4. These tables represent the soil modeling details for the soil strata depicted in Fig. 3.

The boreholes considered in the study were classified based on $V_{S(30)}$ and have been plotted in Fig. 6. Majority of the soil deposits have $V_{S(30)}$ in the range of 350–400 ms^{-1} and that is the boundary between NEHRP 'C' and 'D' site categories. Except for few boreholes belonging to 'C' category, the rest lies in 'D' site class.

4. Selection and scaling of input motions

The generation of input motions for site response analysis consists of three main phases. The first phase involves defining the target spectrum representative of the regional seismic hazard. The second phase deals with the selection of ground motion records compatible with the target spectrum. The third phase involves the modification of the chosen records with respect to the target spectrum. The practice of selecting ground motion varies widely and no definitive guidelines or strict procedures exist. However, the codal provision provides a general guideline to consider a minimum of five recorded or simulated rock outcrop horizontal ground motion records from events of magnitude (M) and distance (R) within the range consistent with those controlling the Maximum Considered Earthquake (MCE) ground motion [37].

In the present study, the Uniform Hazard Spectrum (UHS) derived from PSHA for the said region [7] was modified to obtain the target spectrum. The host to target adjustment of the UHS to obtain target spectrum consistent with the local site condition has been explained in the methodology. The median UHS represents the time varied ground motion parameter resulting from various combinations of magnitude and distances contributing to the seismic hazard for a given POE. The objective of the study is to quantify the seismic site amplification and the UHS resulting from a single hazard level may not be sufficient for developing amplification equation. Hence, multiple hazard levels were considered. The design ground motions specified in the Indian seismic code correspond to 10% POE in 50 years i.e. Design Basis Earthquake (DBE). With DBE as the standard design condition, two more hazard levels i.e., 10*DBE and 0.25*DBE were defined based on the recommendations from Ref. [38]. The DBE (abbreviated as H_M) represents the median hazard level whereas 10* DBE (abbreviated as H_L)

Table 1
Vs – N Correlations investigated in the study.

Authors	Correlation	Soil Type	Region
Maheshwari et al. (2010)[a] - **UM1** [22]	$V_s = 89.31^{a}N^{0.358}$	Clay	Chennai
	$V_s = 100.53^{a}N^{0.265}$	Sand	
	$V_s = 95.64^{a}N^{0.301}$	All Soil	
Hanumanthrao & Ramana (2008) – **HR** [23]	$V_s = 79^{a}N^{0.434}$	Sand	Delhi
	$V_s = 82.6^{a}N^{0.43}$	All Soil	
	$V_s = 86^{a}N^{0.42}$	Silty Sand/'sand' Silt	
Unal Dikmen (2009) – **UD** [24]	$V_s = 58^{a}N^{0.39}$	All Soil	Turkey
	$V_s = 73^{a}N^{0.33}$	Sand	
	$V_s = 60^{a}N^{0.36}$	Silt	
	$V_s = 44^{a}N^{0.48}$	Clay	
Chatterjee & Choudhury (2013)[a] - **CC1** [25]	$V_s = 78.21^{a}N^{0.38}$	All Soil	Kolkata
	$V_s = 77.11^{a}N^{0.39}$	Clay	
	$V_s = 54.82^{a}N^{0.53}$	Silty Sand	
	$V_s = 58.02^{a}N^{0.46}$	Silt	
Kirar, Maheshwari et al. (2016) – **KMM** [26]	$V_s = 100.31^{a}N^{0.348}$	Sand	Roorkee
	$V_s = 94.4^{a}N^{0.379}$	Clay	
	$V_s = 99.5^{a}N^{0.345}$	All Soil	
Maheshwari et al. (2010) - **UM2** [22]	$V_s = 90.75^{a}N^{0.304}$	All Soil	Chennai
	$V_s = 96.29^{a}N^{0.266}$	Sand	
	$V_s = 83.27^{a}N^{0.365}$	Clay	
Hasaneebi & Ulusay (2007)[a] - **NR** [27]	$V_s = 90^{a}N^{0.309}$	All Soil	Turkey
	$V_s = 90.8^{a}N^{0.319}$	Sand	
	$V_s = 97.9^{a}N^{0.269}$	Clay	
Anbazhagan et al.(2012) – **AZ** [28]	$V_s = 68.96^{a}N^{0.51}$	All Soil	Lucknow
	$V_s = 60.17^{a}N^{0.56}$	Sand	
	$V_s = 106.63^{a}N^{0.39}$	Clay	
Sil & Haloi (2017)[a] - **SH** [29]	$V_s = 75.478^{a}N^{0.3799}$	All Soil	Any region
	$V_s = 79.217^{a}N^{0.3699}$	Sand	
	$V_s = 99.708^{a}N^{0.3358}$	Clay	
Mhaske & Choudhury (2011)[a] - **MC** [30]	$V_s = 72^{a}N^{0.4}$	All Soil	Mumbai
Thokchom et al. (2017)[a] - **TK** [31]	$V_s = 2.641^{a}N + 189.6$	Sand	Dholera,
	$V_s = 3.925^{a}N + 143.1$	Silt	Western
	$V_s = 3.395^{a}N + 156.8$	Clay	India.
	$V_s = 3.311^{a}N + 160.5$	All Soils	
Chatterjee & Choudhury (2013) - **CC2** [25]	$V_s = 78.63^{a}N^{0.37}$	All Soil	Kolkata
	$V_s = 78.03^{a}N^{0.38}$	Clay	
	$V_s = 58.62^{a}N^{0.45}$	Silt	
	$V_s = 56.44^{a}N^{0.51}$	Silty Sand	

[a] Correlations used in the study. Nomenclature ending with numbers 1 and 2 represents correlation derived based on uncorrected and corrected SPT 'N' values respectively.

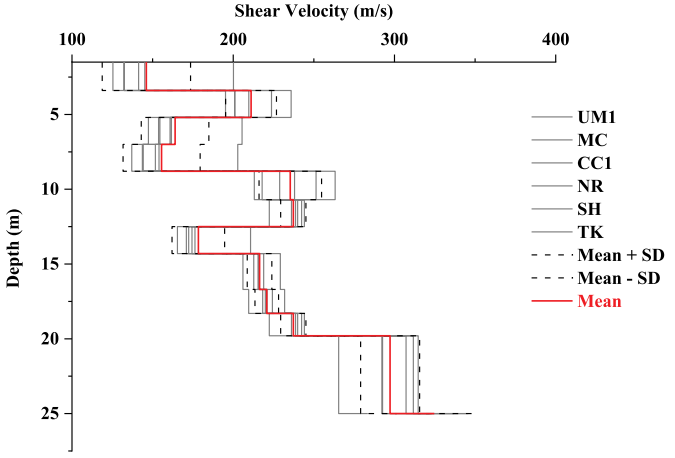

Fig. 5. Shear velocity profile of a typical clay deposit.

and 0.25*DBE (abbreviated as H_H) represents lower and higher hazard levels respectively. H_L correspond to 65% POE and H_H correspond to 2.5% POE in 50 years. The three hazard levels collectively represent the entire scope of regional seismic hazard.

Once the range of the target spectrum was set, the next crucial step was to identify the earthquake scenarios (combination of M and R) controlling the hazard at a site. De-aggregation performed for all the three hazard levels suggested events with magnitude (M_w) in the range of 4–6.5 occurring within a distance of 60 km [7] to be controlling the hazard. The ground motion records were chosen from a similar tectonic regime as that of the study region (i.e. stable continental region) consistent with the de-aggregation findings. Ground motions recorded on a rock site with $V_{S\ (30)}$ corresponding to NEHRP 'B' ($> 760\ ms^{-1}$) had to be considered to be consistent with the site condition of the derived target spectra. With all the aforementioned criteria, the ground motions were selected from the PEER NGA East website and European ground motion database [39]. In order to minimize the uncertainty in ground motion selection, multiple recordings were considered. Studies on the sensitivity of site response analysis to the number of input ground motions reveal at least 10 and preferably 20 ground motions to be considered when incorporating site effects into PSHA [40]. Based on the recommendations [38] and preliminary analysis [41], 11 ground motions for each hazard level summing up to 33 ground motions were considered for each soil column. The details of the ground motion records used in the study are given in Table 5. Few records have been repeated with different scaling factors to match the target spectrum. However, care was taken not to use more than four ground motions from the same event for a given hazard level.

Variety of scaling techniques exists in making the recorded ground motions compatible with the target spectrum. A recent study [42] briefed the impact of different scaling techniques on the overall outcome of site response analysis. In the present study, the recorded acceleration time histories are modified through spectral matching [43] to match the target spectrum at each period using SEISMOMATCH [44]. The scaling factor was limited to 4 and number of iterations to 20 as

Table 2
Input parameters for soil modeling of a site categorized as 'sand'.

Depth, m	Thickness, m	SPT 'N' value	Unit weight kN/m^3	Description	Modulus reduction curve and damping curve
1.5	1.5	1	18.64	filled up earth	SAND, Upper bound (Seed & Idriss, 1970) [32]
3.4	1.9	6	19.62	'sand' clay	
5.1	1.7	25	21.58	laterite	
7	1.9	33	22.56		
10.3	3.3	50	21.58	lateritic clay	CLAY, Upper range (Seed & Sun, 1989) [36]
11.8	1.5	43	19.62	lithormerge	SAND, Upper bound (Seed & Idriss, 1970) [32]
15	3.2	43	20.60		
16.7	1.7	42	19.62	Weathered rock	Rock Fill (Gazetas, 1992) [34]

Table 3
Input parameters for soil modeling of a site categorized as 'All soil'.

Depth, m	Thickness, m	SPT 'N' value	Unit weight kN/m^3	Description	Modulus reduction curve and damping curve
1.5	1.5	4	19.62	Silty Sand	Soil PI = 0 (Vucetic & Dobry) [35]
3.4	1.9	13	20.70	Soft Laterite	
5.2	1.8	6	23.54	Medium Hard Laterite	
7	1.8	5	22.56	Soft Laterite	
8.8	1.8	18	17.17		
10.7	1.9	20	18.54		
12.5	1.8	8	17.56		
14.3	1.8	15	13.44	Silty Sand	
16.7	2.4	16	20.21		
18.3	1.6	20	17.56		
19.8	1.5	39	16.09	Weathered Rock	Rock Fill (Gazetas, 1992) [34]

higher values may alter the ground motion to an extent where the record may lose its original nonstationary characteristics. The comparison of the target spectrum along with the scaled records and mean matched spectrum is shown in Figs. 7–9. Since median UHS was chosen for the study, a slightly flexible range of scaled ground motions have been considered to represent varied input acceleration values.

5. Methodology

The shear velocity profile was estimated for each bore log by considering the average of the various V_S–N correlations. One of the major drawbacks of using SPT tests to determine V_s is that the borehole terminates upon reaching refusal strata. But the V_S of this refusal can be as less as 320 ms^{-1} and the engineering bed layer (EBL) is characterized by a $V_{S(30)}$ of 760 ms^{-1}. Based on the findings from the earlier mentioned literature in section 2, it was found that the depth to bedrock varied between 15 m and 50 m. Due to the presence of weathered and fractured rock in the strata, refusal was met at a very shallow depth between 15 m and 25 m. For the purpose of modeling the soil columns for numerical simulations, the depth to EBL was assumed as 50 m from the surface.

The input motions for site response analysis are usually scaled to match the UHS obtained from PSHA. However, in the present case, the UHS developed earlier was for a reference site (V_S > 1500 ms^{-1}) differing from the local site condition at the base of the soil column. The applied input motions need to be consistent with the soil conditions at the base of the soil profile i.e EBL. Hence, the target spectrum required the host to target adjustment (HTTA), wherein the UHS is modified to represent the local site condition. The HTTA is usually performed using $V_{S(30)}$ and κ_0 (site-specific attenuation parameter) estimating large high-frequency motion on hard rock compared to standard rock. In the absence of site-specific values of κ_0, suitable $V_{S(30)}$ - κ_0 correlation can be used. However, recent studies have highlighted that these correlations are not robust [45] and the measurement of κ may be biased by site amplification resulting in site effects accounted twice [46]. Further, it was found that this methodology is associated with a high level of uncertainty as explained by Ref. [47]. The absence of field recordings for the study area and the demerits associated with the existing HTTA

Table 4
Input parameters for soil modeling of a site categorized as 'clay'.

Depth, m	Thickness, m	SPT 'N' value	Unit weight kN/m^3	PI	Description	Modulus reduction curve and damping curve
0.9	1.5	7	20.60	23	'clay' Sand (Yellow)	CLAY (PI = 20–40, Sun et al., 1988) [33]
3	2.1	18	19.62	27	Stiff clay Yellow	
7.6	4.6	2	16.87	40	Clay (Yellow)	
10.6	3	5	15.01	37	Clay with Organic matter	
14.7	4.1	5	15.50	–	Clay (grey)	CLAY, Upper range (Seed & Sun, 1989) [36]
18.6	3.9	6	15.70	50	Clay	CLAY (PI = 40–80, Sun et al., 1988) [33]
21.6	3	9	16.68	–		CLAY, Upper range (Seed & Sun, 1989) [36]
24.4	2.8	50	19.52	20	Lateritic Soil	CLAY (PI = 20–40, Sun et al., 1988) [33]
30	5.6	24	15.79	49	Silty clay	CLAY(PI = 40–80, Sun et al., 1988) [33]
32.6	2.6	20	15.30	53		
37	4.4	17	14.72	–	Clay mixed with Quartz	CLAY, Upper range (Seed & Sun, 1989) [36]
38.1	1.1	50	14.72	–	'sand' Clay	
41.1	3	19	14.72			
44.8	3.7	48	19.62	–	Weathered Rock	Rock Fill (Gazetas, 1992) [34]

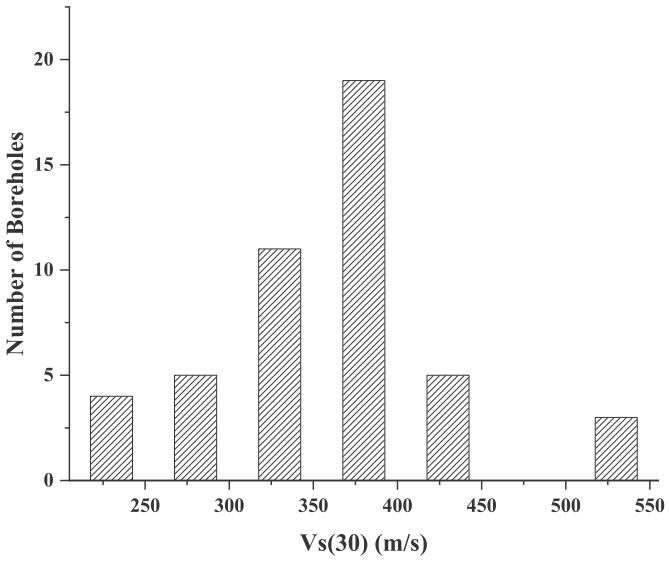

Fig. 6. Histogram of the number of soil profiles simulated in the study.

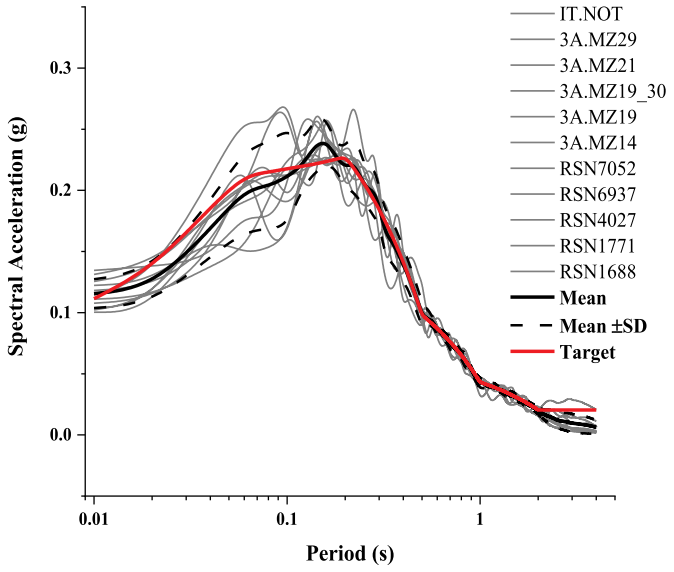

Fig. 7. Plot of 5% damped rock acceleration spectrum of ground motions scaled to H_M.

procedures led to the use of a simpler and straightforward approach. It is a common understanding that the amplification phenomena is primarily controlled by the velocity contrast between the rock and soil. Using this approach, recently a GMPE was proposed [48] (abbreviated as LA13) using surface and in-depth recordings of Japan, wherein the site term relied on the V_s alone. This methodology has an advantage as the site response in itself was recorded and not simulated. The empirically derived amplification ratio is given as

$$HTTA\ factor = \frac{Soft\ rock\ (760\ ms^{-1})}{Hard\ rock\ (1500\ ms^{-1})}(T) = \exp(C_1(T) * \ln\left(\frac{760}{1500}\right)) \quad (1)$$

The coefficient C_1 is estimated from the actual recordings for each spectral period T. It seems questionable about the applicability of amplification factors developed elsewhere for regional conditions.

Table 5
Details of ground motions used in the study.

Earthquake name	Acronym	Date	Mw	R_{rup} (km)	$V_{S(30)}$/Site class	PGA (g)	Scaled PGA	Hazard level
RiviereDuLoup	RSN1688	06-03-2005	4.65	19.05	2000	0.045	0.100	**Median hazard level, H_M**
RiviereDuLoup	RSN1771	06-03-2005	4.65	41.75	1026	0.070	0.124	
Greenbrier	RSN6934	28-02-2011	4.68	6.27	1403	0.030	0.135	
Greenbrier	RSN7052	28-02-2011	4.68	54.07	1288	0.001	0.126	
ValDesBois	RSN4027	23-06-2010	5.1	52.94	1700	0.018	0.102	
Sicily	IT.NOT	13-12-1990	5.6	48.30	A	0.090	0.111	
Central Italy	3A.MZ14	26-10-2016	5.9	36.60	A	0.515	0.108	
Central Italy	3A.MZ19	26-10-2016	5.9	30.40	A	0.096	0.118	
Central Italy	3A.MZ21	26-10-2016	5.9	30.70	A	0.183	0.104	
Central Italy	3A.MZ19_30	30-10-2016	6.5	22.60	A	0.363	0.114	
Central Italy	3A.MZ29	30-10-2016	6.5	26.90	A	0.689	0.131	
RiviereDuLoup	RSN1688	06-03-2005	4.65	19.05	2000	0.045	0.172	**Higher hazard level, H_H**
RiviereDuLoup	RSN1771	06-03-2005	4.65	41.75	1026	0.070	0.237	
ValDesBois	RSN4027	23-06-2010	5.1	52.94	1700	0.018	0.174	
Greenbrier	RSN6934	28-02-2011	4.68	6.27	1403	0.030	0.231	
Greenbrier	RSN7052	28-02-2011	4.68	54.07	1288	0.001	0.227	
LaMalbaie	RSN1199	13-06-2003	3.53	10.06	2000	0.056	0.205	
LaMalbaie	RSN1192	13-06-2003	3.53	52.75	2000	0.000	0.218	
Central Italy	3A.MZ11	26-10-2016	6.5	24.8	A	0.044	0.170	
Central Italy	IT.ACC	26-10-2016	6.5	18.6	A	0.090	0.172	
Sicily	IT.NOT	13-12-1990	5.6	48.3	A	0.090	0.214	
Sicily	IT.SRT	13-12-1990	5.6	36.9	A	0.107	0.180	
L'Aquila	IT.ANT	06-04-2009	6.1	26.2	A	0.01974	0.02261	**Lower hazard level, H_L**
L'Aquila	IT.LSS	06-04-2009	6.1	41.5	A	0.00961	0.01913	
L'Aquila	IT.SUL	06-04-2009	6.1	53.7	A	0.03362	0.02296	
Sicily	IT.NOT	13-12-1990	5.6	48.3	A	0.08865	0.02538	
Sicily	IT.SRT	13-12-1990	5.6	36.9	A	0.10536	0.02634	
Bovec	RF.SVAL	12-04-1998	5.7	23.5	A	0.02492	0.01958	
Bovec	RF.MOG	12-04-1998	5.7	40.5	A	0.01508	0.02462	
RiviereDuLoup	RSN1681	06-03-2005	4.65	39.01	2000	0.02125	0.02327	
ValDesBois	RSN4027	23-06-2010	5.1	52.94	1700	0.04829	0.0276	
Central Italy	3A.MZ11	26-10-2016	5.9	31	A	0.04324	0.01924	
Central Italy	3A.MZ14	26-10-2016	5.9	36.6	A	0.05053	0.02712	

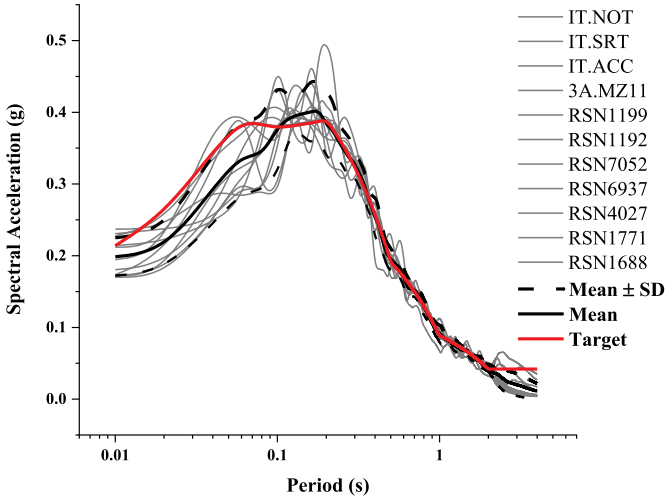

Fig. 8. Plot of 5% damped rock acceleration spectrum of ground motions scaled to H_H.

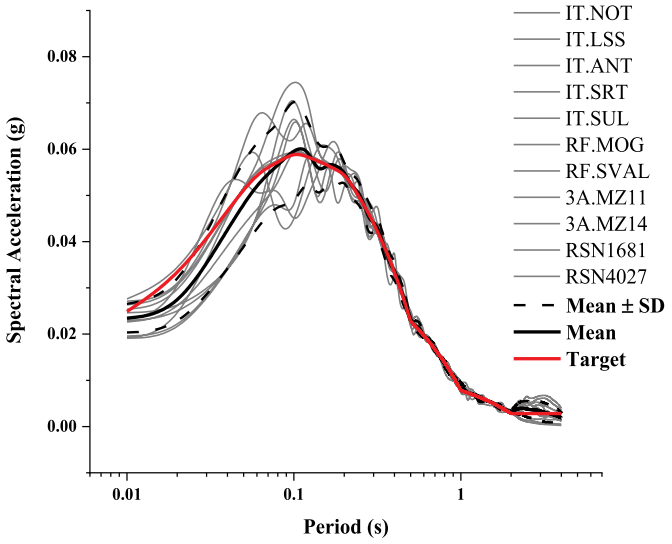

Fig. 9. Plot of 5% damped rock acceleration spectrum of ground motions scaled to H_L.

However, most of the seismic hazard studies use nonlinear amplification function developed using California and other active region data [49]. At least the presently used amplification factor was derived based on actual recordings without any prior assumption about unmeasured parameters such as κ_0. The UHS is multiplied with the HTTA factors to obtain the target spectrum consistent with the site conditions at the base of the soil profile. The ground motions are then scaled to the adjusted UHS (termed as target spectrum in Figs. 7–9) and used as input motion for site response analysis. The UHS from PSHA and the target spectrum computed by performing HTTA are presented in Fig. 10 for the three distinct hazard levels considered in the study.

The actual site respose is a combination of local site response, basin and topographic effects which cannot be captured by 1D propagation of shear waves alone. However, when topographic and basin effects are not significant 1D site response analysis can be computed. The approach is based on the assumption that the site response is dominated by the vertically upward propagating seismic shear waves from the underlying rock formation. The site response analysis was performed using an equivalent linear approach (EQL) to model nonlinear behavior of soils on SHAKE2000 platform. Studies have revealed that EQL is efficient for stiff soils subject to weak motions with PGA < 0.4 g and maximum induced shear strain is less than 0.3% [50].The site response analysis requires input parameters representing the soil dynamic characteristics in the form of backbone and damping curves. The averaged shear velocities over the depth of the soil column and unit weight of each layer constituting the soil column are considered in estimating the shear modulus G_{max}. The equivalent linear approach estimates the backbone curve by combining the computed G_{max} and the designated *M*-R curves (Tables 2–4) for each distinct subsurface material.

$$G_{max} = \rho * V_s^2 \tag{2}$$

The EQL method uses an iterative procedure to compute strain compatible secant moduli (G) and damping (D). The iteration converges when the difference in the computed parameters in two successive iterations is less than 5%. However, these parameters are time-invariant and are assigned to each soil layer. The geological formation below the base of the soil profile is modeled as elastic half space and the scaled records are applied as outcrop motion at the base.

The local site effects on the transmitted ground motion have been captured in the form of amplification equation at varying natural frequencies (f)/periods (AF(f)). The study highlights the influence of local soil characteristics in ground motion amplification and suggests that $V_{s(30)}$ alone is not sufficient in capturing the local site amplification. Hence, the amplification factor has been derived as a function of input rock motion for different periods. Initially, the amplification factor and its corresponding input rock spectral acceleration were plotted. A careful study of the scattered plot (shown in Figs. 13–15) suggested that a linear fit may not effectively capture the displayed nonlinear behavior. Hence, a nonlinear regression (of the form in equation (3)) was performed.

$$\ln AF(f) = a + b * \ln(S_a^r(f) + c) + \varepsilon_{\ln AF(f)} * \sigma_{\ln AF(f)} \tag{3}$$

The coefficients a,b, and c are obtained from the regression between the amplification factor (AF) and adjusted rock spectral acceleration (S_a^r) in logarithmic space. The term $\sigma_{\ln\ AF(f)}$ represents the standard deviation in the estimated AF values from nonlinear regression and $\varepsilon_{\ln\ AF(f)}$ is the standard normal variable. The procedure has been repeated for different spectral periods such as T = 0.01s (PGA), 0.2s, 0.8s, 1s, 1.5s, and 3s and for different site categories. Physically, the coefficient 'a' represents weak site amplification, 'b' represents nonlinearity of the soil and 'c' represents the threshold value of the input rock spectral acceleration (S_a^r(f)) below which the amplification becomes linear. The input motions from multiple hazard levels result in a wide range of input values (S_a^r(f)) and regression is poorly constrained by coefficients. It is a common practice to constrain one or more coefficients ('a' and 'c') to provide a good fit. During curve fitting, it was observed that the coefficient 'c' was poorly constrained with a high estimation of uncertainties. Hence, the coefficient 'c' was initially set based on visual inspection of the scatter plot and subsequently modified based on trial and error. A value of 0.05 seems to fit well for all the three site categories at T = 0.01s. The coefficients a, b and c estimated for all the three site categories along with their standard error are shown in Fig. 11.

In order to obtain hazard consistent amplification factor, the amplification ratio (AF′(f)) must be computed between the ground motion parameter at the surface and the reference site condition for which hazard was computed.

$$\ln AF'(f) = \ln AF(f) + \bar{Y} \tag{4}$$

$\bar{Y}$ represents the median amplification between the reference site condition and the base of the soil profile computed from an ergodic site amplification model (in the present case, it is LA13 site amplification model). Accordingly, the input motion at the base of the soil profile is modified as

$$\ln S_a^{r'} = \ln S_a^r - \bar{Y} \tag{5}$$

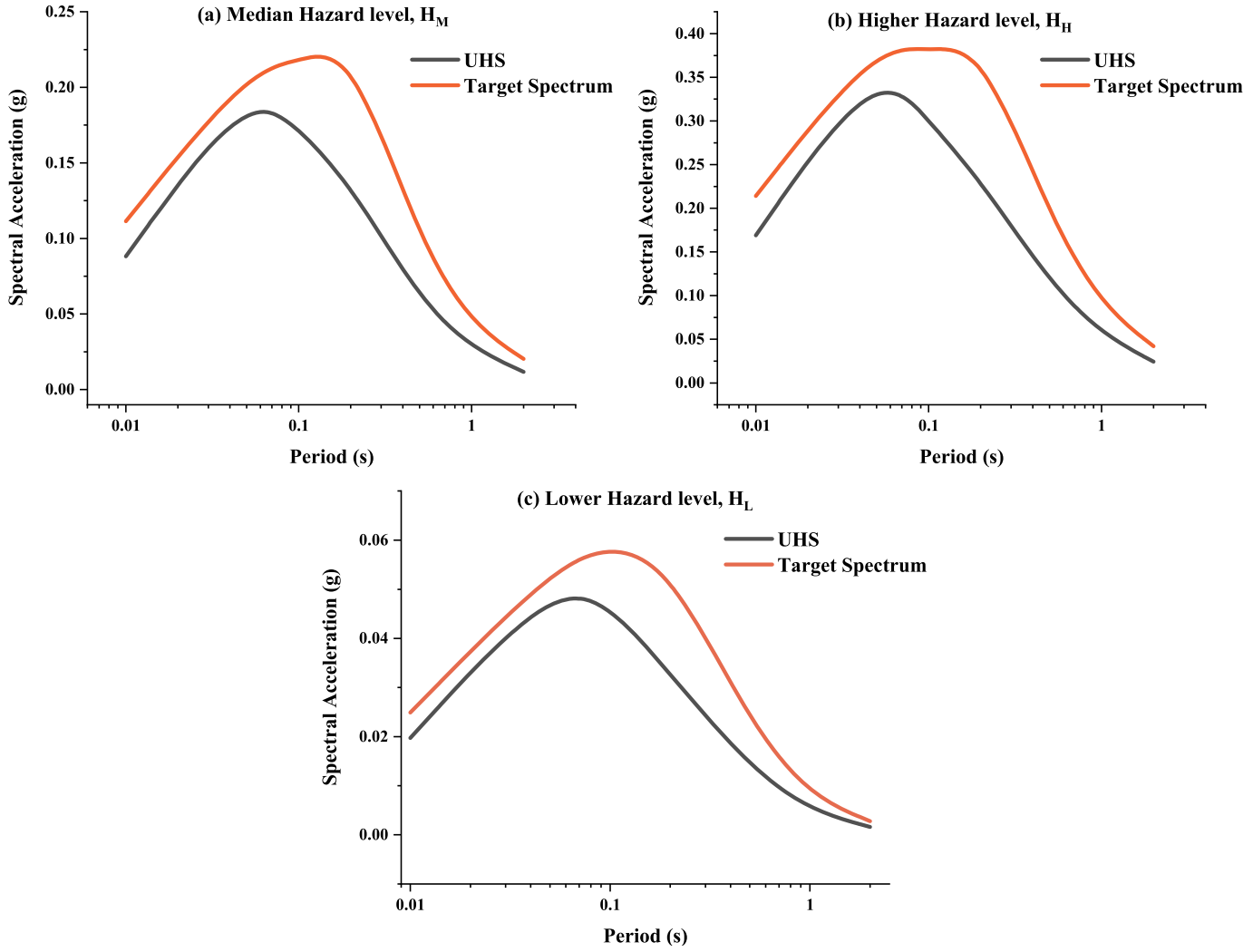

Fig. 10. Plots depicting the UHS obtained from the earlier PSHA study and the modified UHS termed as 'Target Spectrum'.

The developed nonlinear amplification model was integrated with the existing rock GMPE, hence, transforming it into a site-specific GMPE. A closed form equation was proposed for transforming the GMPE [5].

$$ln\overline{S_a^s(f)} = \ln \overline{S_a^{r'}(f)} + \ln AF'(f) \tag{6}$$

The terms $\overline{S_a^{r'}(f)}$ and $\overline{S_a^s(f)}$ represents median reference rock and surface spectral acceleration respectively. One of the advantages of this transformation is that the variability in the resulting surface hazard can be captured. The standard deviation term for the surface hazard considers the variability in the rock hazard as well as site amplification [51].

$$\sigma_{\ln S_a^s(f)} = \sqrt{\left(\frac{b * S_a^r(f)}{C + S_a^r(f)} + 1\right)^2 * \sigma^2_{\ln S_a^r(f)} + \sigma^2_{\ln AF(f)}} \tag{7}$$

The adopted methodology offers an advantage of transforming a generic GMPE by performing site response analysis with lesser ground motions as compared to that required to develop a site-specific GMPE.

6. Results and discussion

The compiled borehole information along with the selected and scaled input motions served as input to equivalent linear analysis. The dynamic characteristics of the local soil are explained through different output parameters such as amplification and surface response spectrum. Due to space constraint, the results of all the simulated soil columns are not considered. Instead, three representative soil profiles having shear velocity (Vs $_{(30)}$) in the range of 331–332 ms^{-1} were chosen. Fig. 12 represents the 33 amplification functions derived from the selected ground motions for the three chosen sites. It is interesting to note that two wide peaks are observed at 0.12s–0.16s and 0.28s–0.36s in all the three cases. The 'sand' site amplifies the ground motion at the bedrock by a factor of 4.64 near to its predominant site period of 0.33s. However, in spite of having the same Vs $_{(30)}$, a higher spectral amplification of 5.52 was observed at 0.36s for all soil site. A 'clay' site with Vs $_{(30)}$ of 331 ms^{-1} produces the surface motion amplified 7.05 times the input motion at 0.28s. The significant difference in site amplification among the three considered profiles highlights the drawback of generic site amplification factors based on Vs $_{(30)}$ to capture the soil dynamic characteristics. In all the cases, higher variability was observed close to the first two soil resonant frequencies (i.e. first two peaks) and PGA. Relatively higher variability was observed in 'clay' deposits representing the large differences in the intensity of input motions.

The amplification characteristics of all the simulated soil profiles are presented in three different categories based on the predominant soil type. Fig. 13 represents the median amplification function along with the standard deviation and 95% confidence interval as a function of rock spectral acceleration assessed at different spectral periods. The amplification function varying with the period (AF(f)) for different input motion acceleration values (PGA and S_a (f)) was compiled for all the numerically modeled soil deposits belonging to 'all soil' site

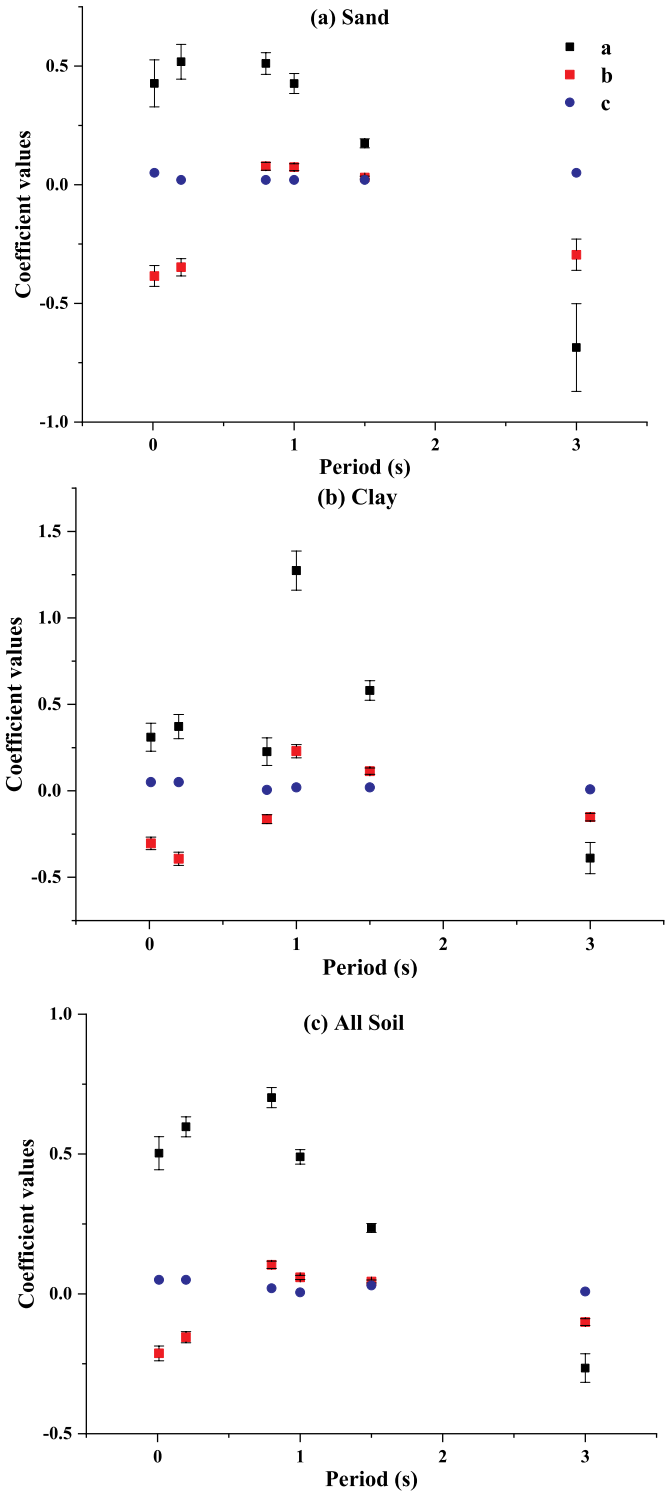

Fig. 11. Coefficients from nonlinear regression.

category. Each soil profile generated 33 data points from the input ground motions for each period window. The plots for T = 0.8s, 1s, and 1.5s clearly distinguish the difference in the input ground motion scaled corresponding to three different hazard levels.

At T = 0.01s (PGA) and 0.2s, the amplification observed is higher compared to other periods. Additionally, the nonlinear behavior of the soil is well represented in these two periods. The natural site period of the analyzed soil columns lies in the range of 0.3–0.5s. However, at T = 0.8s, 1s and 1.5s the trend of the fitted curve changes from a

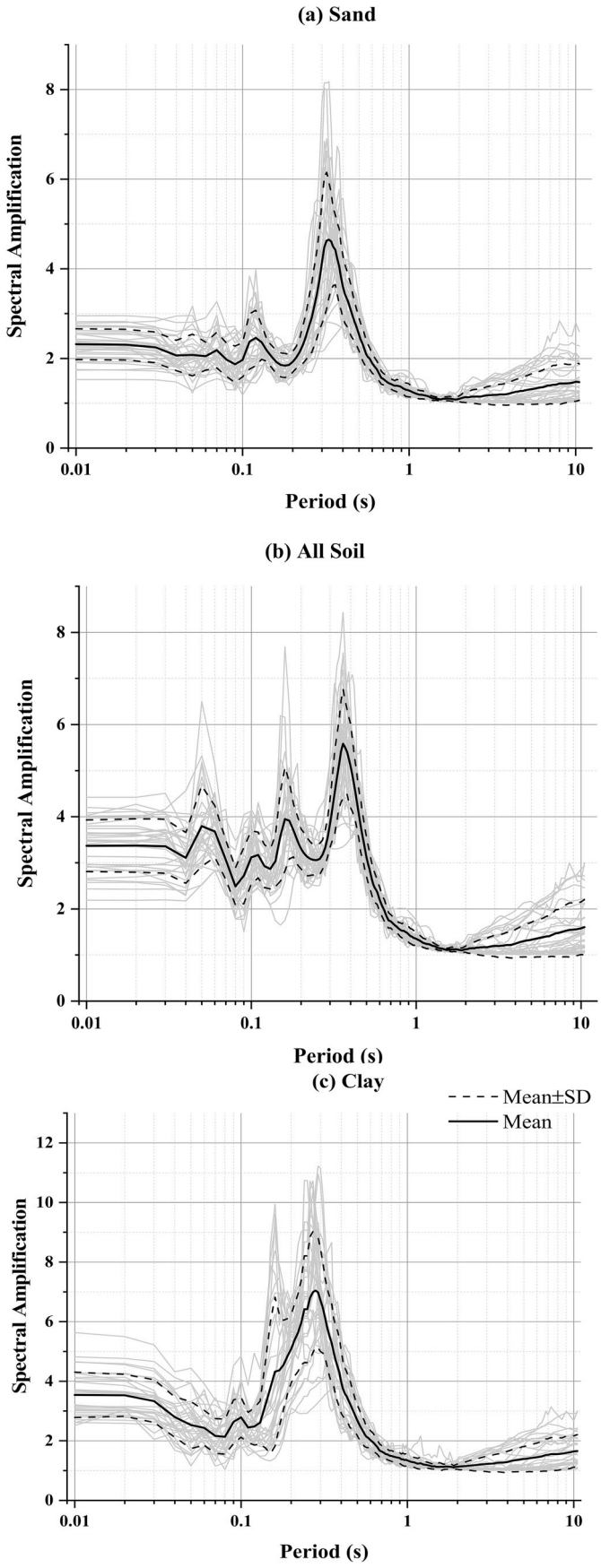

Fig. 12. Spectral Amplification for **a.** 'sand' site **b.** All soil site **c.** 'clay' site.

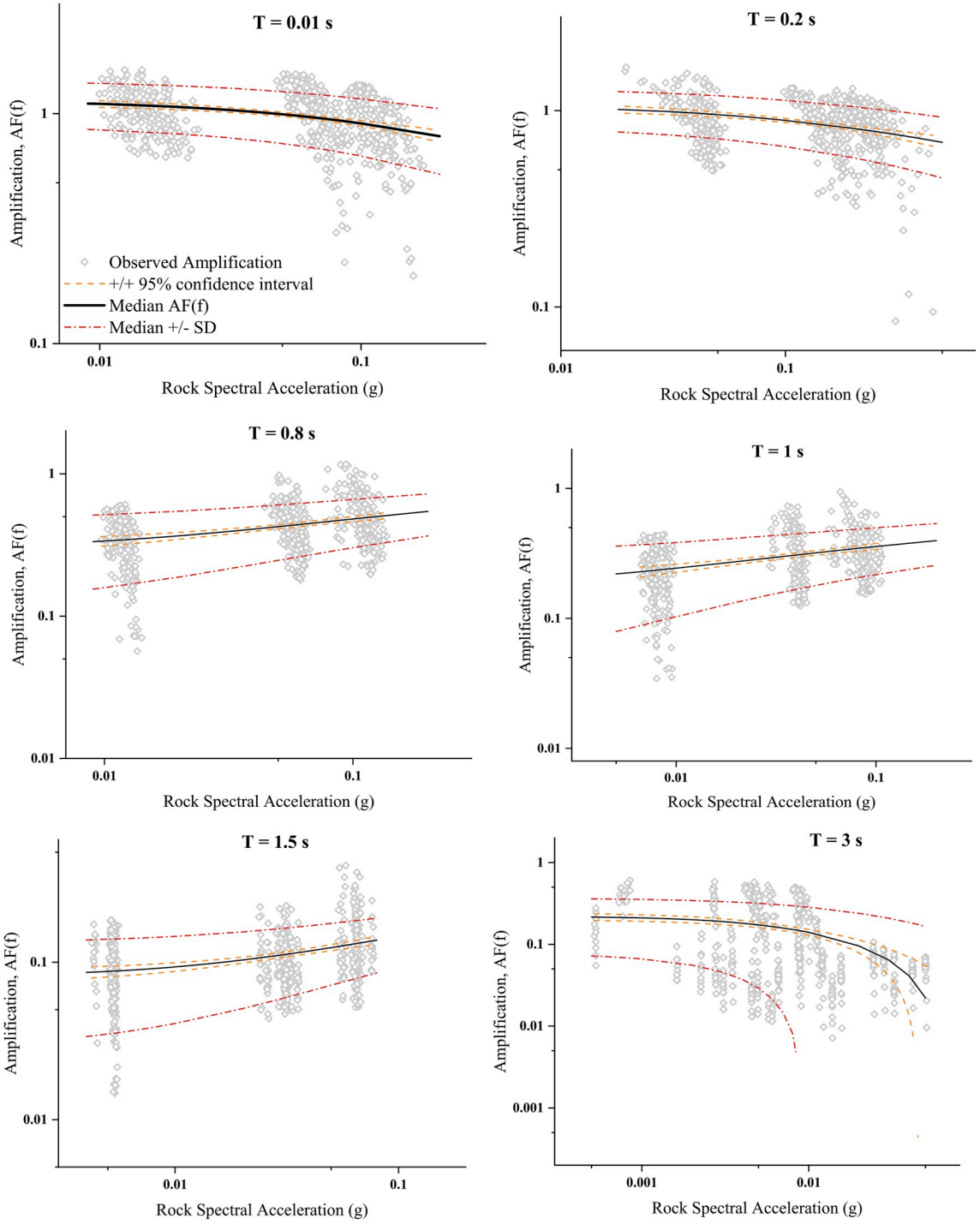

Fig. 13. Amplification factors regressed against rock spectral acceleration for 'all soil' sites.

negative slope to positive slope and is characterized by lower amplification factors. It can be inferred that a negative correlation exists at periods below the fundamental site period. The nonlinear regression coefficients obtained for T = 3s is not statistically significant as evident from the bottom right panel of Fig. 13. Though the values of AF(f) are considerably less, sustained amplifications are observed at longer periods implying that the site characteristics are critical for longer period ground motions.

Fig. 14 represents the amplification functions derived for 'sand' site for different spectral periods. The observed amplification data points are sparse and widely distributed in comparison with the previous plot due to a lesser number of simulated soil profiles. However, they were sufficient to draw a nonlinear amplification function for different spectral periods. The natural period of the soil profiles lies in the range of 0.31s–0.38s. The depicted soil type i.e. sand tends to be highly nonlinear especially at periods below the average site period. Significant variability is visible for higher spectral acceleration values at T = 0.02s, demonstrating larger variation at T = 0.8s, 1s, and 1.5s. This is mainly due to the large differences in intensity of the selected input ground motions as evident from Figs. 7–9. Similar to the previous Fig. 13, an upward shift was observed at intermediate and longer period range (T = 0.8s–1.5s). The inability of the equivalent linear methodology to converge to a solution for high-intensity records is the reason behind this upward shift [52]. Additionally, the equivalent linear

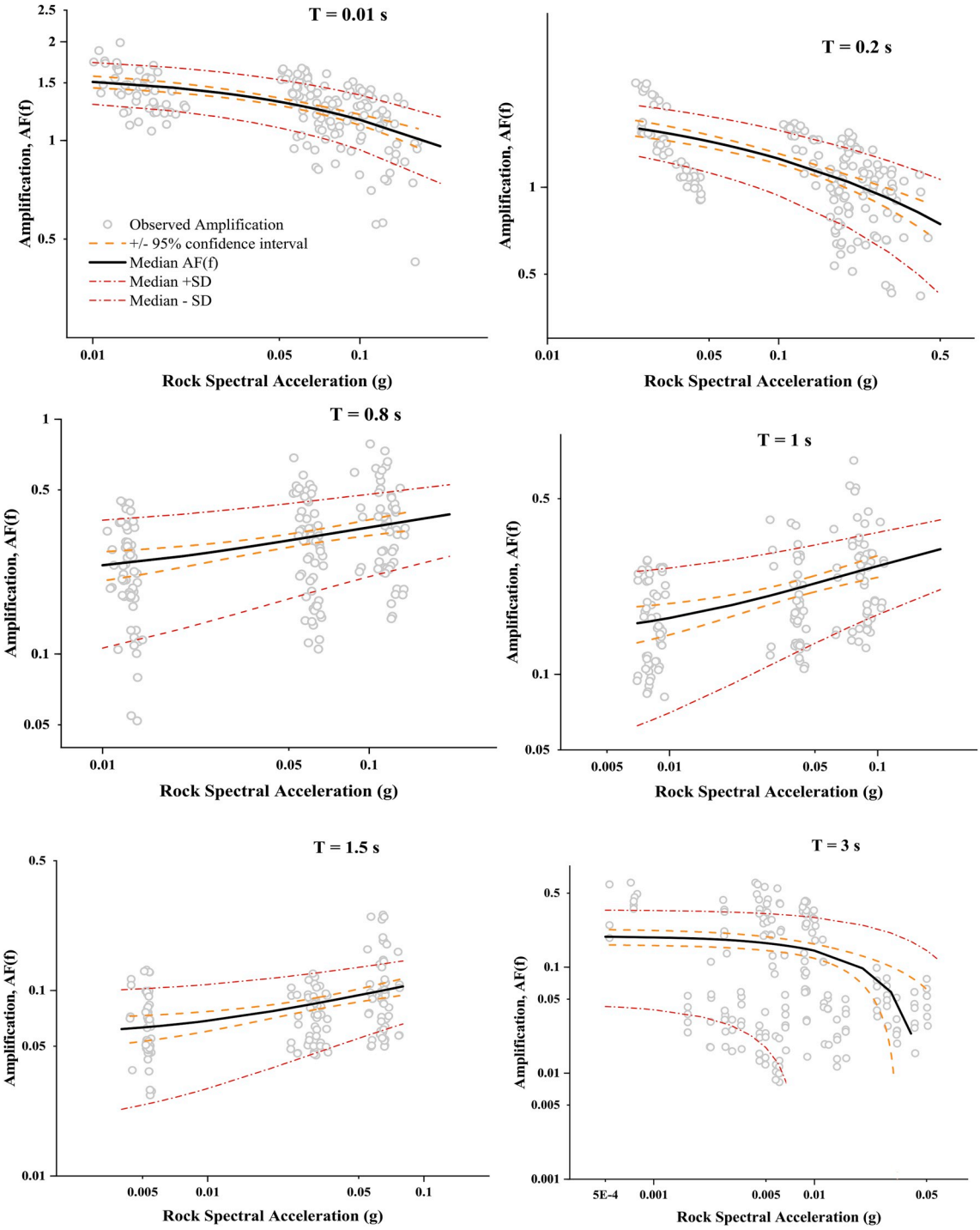

Fig. 14. Amplification factors regressed against rock spectral acceleration for 'sand' sites.

method estimates higher amplification at smaller period range and overestimates resonant responses when the soil becomes nonlinear [50]. Further, the amplification reduces drastically for periods after the resonant vibration period of the sites.

Another interesting observation made during the study is the shift in the natural period depending on the strain induced by various ground motions. In order to explain this phenomenon, a typical 'sand' site with a predominant period of vibration of 0.33s was considered (Fig. 12). Ground motions with lower PGA values especially scaled to H_L indicated a lower period of vibration in the range of 0.317s–0.319s. On the other hand, ground motions scaled to H_H indicated a higher period of vibration in the range of 0.348s–0.358s. Though the shift from the predominant period of vibration is small for the considered ground motions, a higher shift can be witnessed in the case of ground motions with higher acceleration values.

Fig. 15 depicts the nonlinear regression in logarithmic space between amplification factor and input rock spectral acceleration for 'clay'. The amplification observed at T = 0.01s and 0.2s is less when compared with 'sand' deposit. However, the 'clay' sites have demonstrated sustained amplification at longer periods (T = 1s and 1.5s). While the majority of the soil deposits have their natural period around 0.4s, there are few deposits with a period as high as 0.7–0.9s displaying a diverse range. However, the shift in the natural period depending on the induced strain was noticed similar to the 'sand' site. Due to this

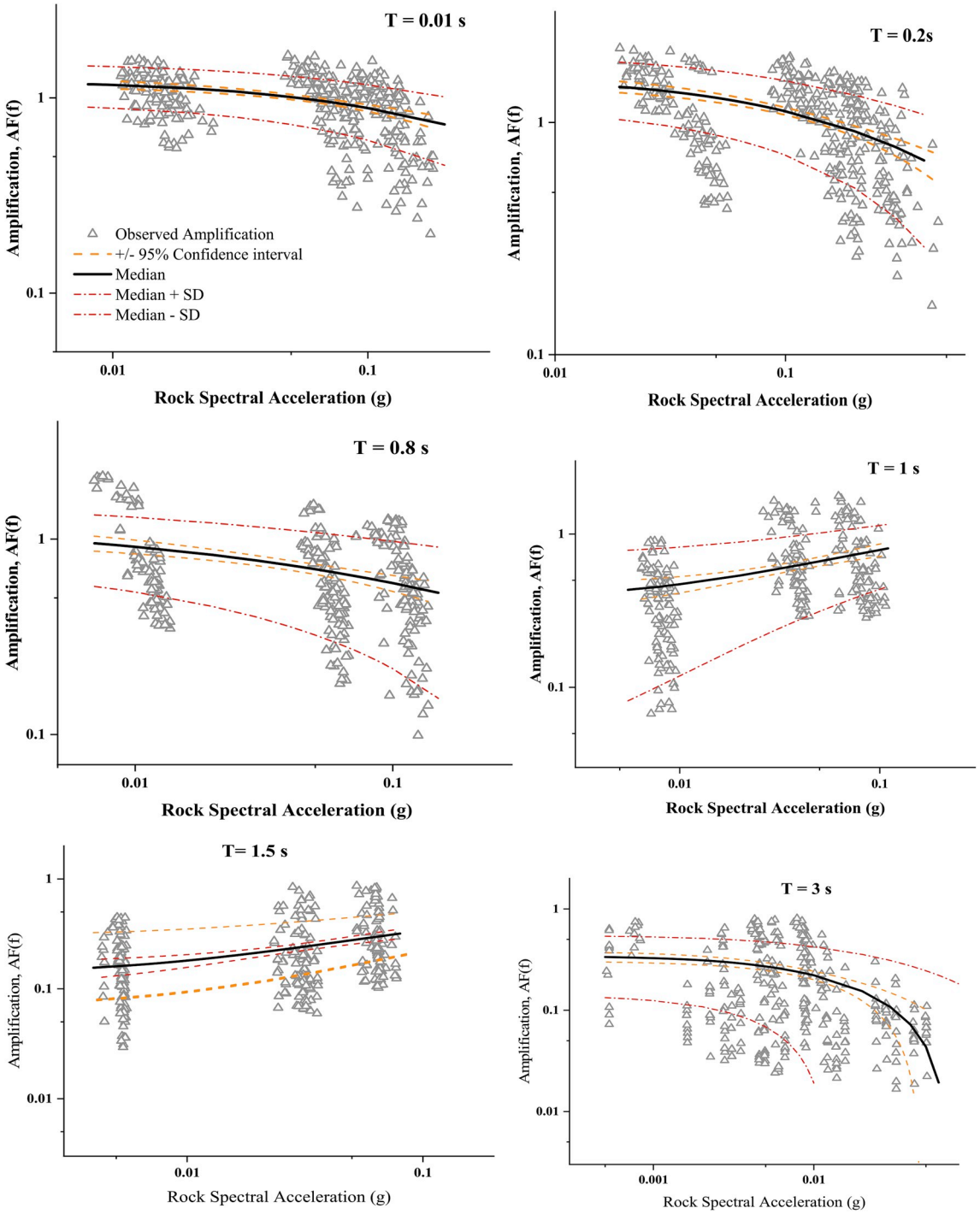

Fig. 15. Amplification factors regressed against rock spectral acceleration for 'clay' sites.

phenomena, resonance is attained by soil profiles at the elongated site period (T = 0.8, 1s and 1.5s) driving the regression towards a positive correlation. As a result, the upward shift in the fitted median amplification curve was observed at these periods. The 'clay' deposits exhibit stronger linearity compared to 'sand' deposits by producing higher amplification at T = 0.8s. The 'clay' site demonstrated consistently higher AF(f) compared to other two site categories implying amplification of longer period ground motions. Overall, 'clay' sites demonstrate slower stiffness degradation and hence, less nonlinear when compared to 'sand' sites.

The nonlinear regression of amplification factors against rock spectral acceleration provides a mean value as well as the variability between the observed value and the fitted mean value. This variability commonly referred to as the standard deviation for the three site categories investigated in the study has been shown in Fig. 16. The standard deviation of the 'all soil' site seems to be lower compared to the other two over the entire period range. A large number of soil profiles considered under this category tends to have reduced the overall variability. However, the highest value of 0.28 was observed in 'clay' (T = 0.01s) and 'sand' (T = 0.2s) type sites at the different yet lower spectral period. The general trend of the curves suggests that the standard deviation is high for periods below the site periods and drops drastically for greater periods. It is important to note that the standard deviation does not exceed 0.3, in agreement with the findings of [53].

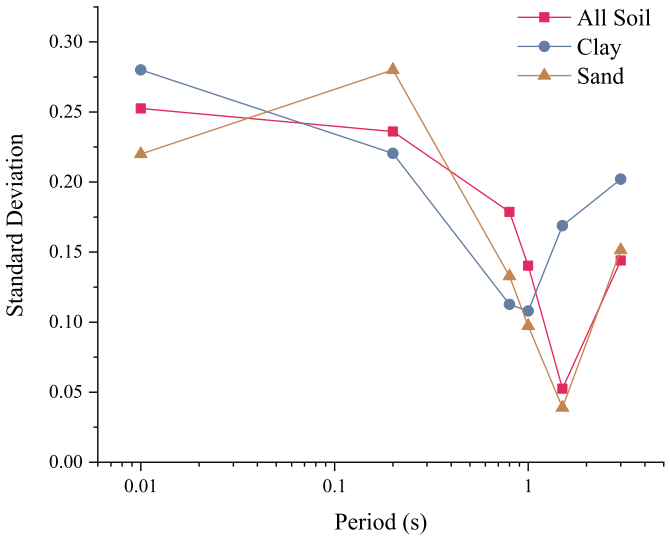

Fig. 16. Plot of the standard deviation of the derived amplification function.

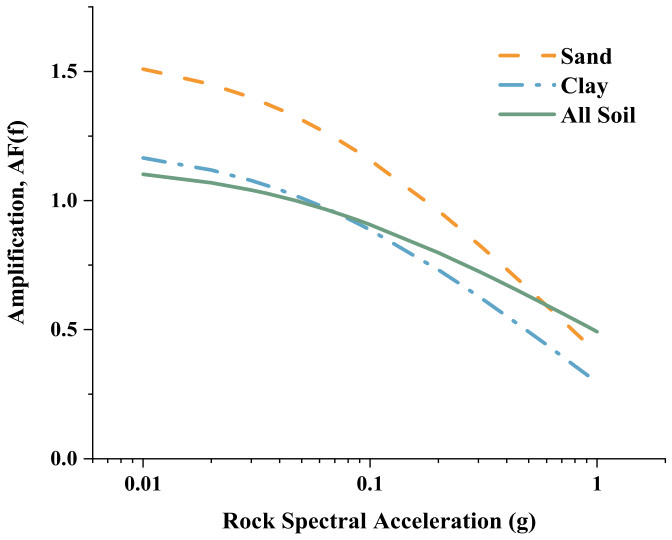

Fig. 18. Mean site amplification of all three soil types at T = 0.01s.

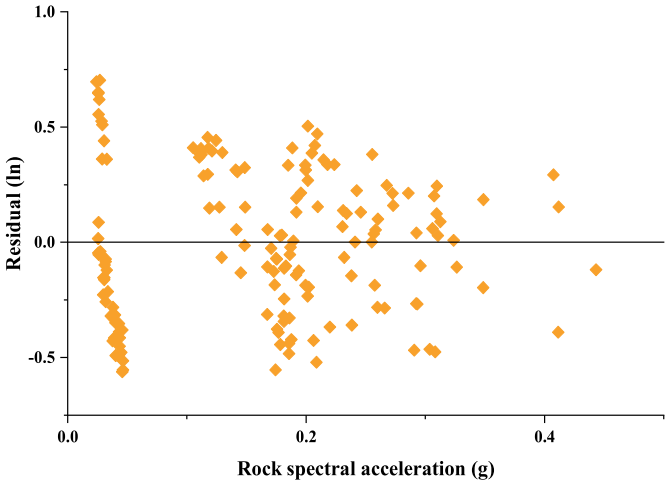

Fig. 17. Residual plot of fitted AF(f) with respect to S_a (0.2s) for 'sand' type.

As higher variability was observed in 'sand' deposit at T = 0.2s, the residual plot for the same has been presented in Fig. 17. The ground motion records scaled to H_L tend to have acceleration value (S_a(0.2s)) in the range of 0.3 g, due to which huge overlapping of the ordinates can be seen. However, the amplification varies slightly, moving the X ordinate about the same Y ordinate leading to higher residuals in the fit. This can be balanced by choosing ground motions with varied acceleration values as evident in input values S_a(0.2s) > 0.2 g. Another interesting observation is that the nonlinear curve fits well at higher acceleration values demonstrating strong nonlinearity in 'sand' soils.

The shear wave velocity in top 30 m is widely accepted as an index for soil amplification. However, the present study suggests that the soil characteristics affect the amplification to a greater extent. In order to validate this, three profiles of same $V_{s(30)}$ but of different soil type are considered for plotting mean amplification in Fig. 18. As evident from Fig. 18, the sand exhibits higher amplification at lower input values but decreases gradually with the increase in PGA demonstrating its nonlinear behavior. For the 'clay' site, amplification reduces as the intensity increases and de-amplification can be noticed for PGA values as small as 0.005 g. However, there is still a very clear amplification at longer periods as shown in Fig. 15. An important observation made during the analysis of 'clay' deposits is that as the soil plasticity index increases the behavior of the soils became less nonlinear. The overall amplification is lesser in All soil type when compared to other two soil types. However, the amplification does not substantially reduce for higher PGA values implying less nonlinearity in the soil sediment.

The fluctuation in the recorded acceleration values at the interface of each constituent layer in a soil profile has been shown in Fig. 19. The PGA at the bottom of the soil profile is almost the same for the three distinct soil types. As the propagation progresses through various soil layers toward the surface the transmitted ground motion undergoes modification consistent with the dynamic characteristics and the same is evident from Fig. 19. The three soil types with the same shear velocity are still dependent on the other soil characteristics in modifying the behavior of the ground motion. Maximum amplification can be observed in the 'clay' deposit for a smaller depth. A similar trend has been followed by the all soil type but amplification becomes significant in the top 10 m. In the case of 'sand' deposit, a gradual amplification was observed with the top 6 m being crucial in altering the PGA value. The PGA values at the surface are 0.21 g, 0.15 g, and 0.20 g for clay, sand and all soil respectively. The careful examination of each ground motion record along the depth revealed that records with PGA < 0.1 g tend to produce higher amplification when compared to records with PGA > 0.2 g. It is mainly due to the fact that as the intensity of the applied motion increases the nonlinear behavior of the soil becomes predominant and dampens the observed surface PGA. The strong nonlinearity of the 'sand' sites as observed in Fig. 14 tends to reduce the intensity of the ground motion at the surface.

The site-specific seismic hazard analysis was performed by transforming the GMPE to include developed site amplification equation for various spectral periods. The hazard curves have been compared for two different spectral periods for varying site condition in Fig. 20. At T = 0.01s, the surface level hazard curve can be seen distinctly varying from that of rock at lower spectral acceleration values. However, as PGA increases beyond 0.3 g, trend tends to be diminishing and closely merging towards the rock hazard curve. This behavior is mainly due to the fact that the amplification equation was derived as a function of input motion at the bedrock level, which in turn induces the strong nonlinear effect. At T = 1s, the intensity values are lower and as a result, the nonlinear effect is minimal. Hence, the difference in the estimated intensity values between the two site conditions for T = 1s is greater than the same at T = 0.01s.

The computed surface UHS was compared with the elastic spectrum recommended by various codes as well as the target spectrum as shown in Fig. 21. The soft soil condition was taken for computing the spectra from Indian code [1]. The code underestimates the amplification potential of regional soils and hence cannot be used for site-specific applications. A similar comparison was made with [53] by choosing the

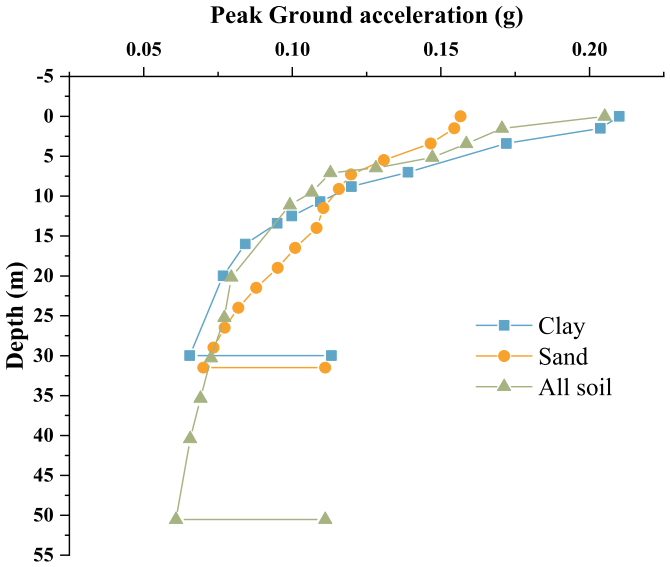

Fig. 19. Plot of variation of PGA along the depth of the soil profile for different sites.

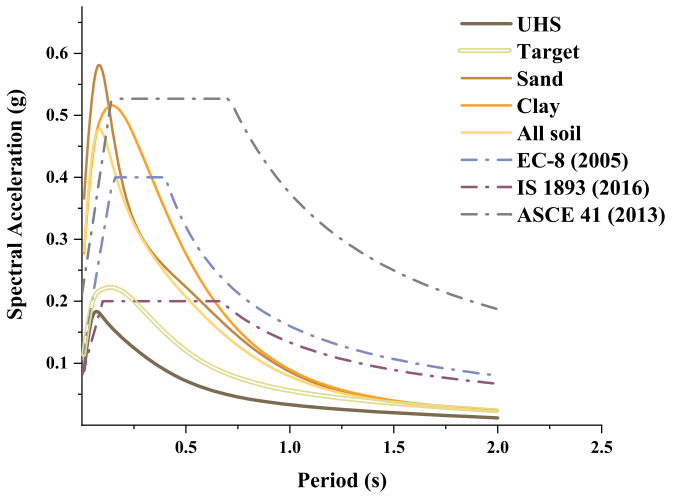

Fig. 21. Comparison of site-specific spectra obtained from the study with that of the codal provisions and the target spectrum.

ground type as 'C' and importance class as II for generating the site-specific spectra. The codal provision underestimates the spectral values at smaller periods (T < 0.5s) and overestimates at higher values. A similar observation was made when compared with the ASCE [54] elastic spectrum for soil class D. However, the ASCE spectrum provides a better estimation and captures the site amplification reasonably well among the three codal provisions. The lower estimation of the spectra resulting from the study for a certain period range may be due to over damping by EQL analysis. As expected the 'sand' site provides higher spectral acceleration followed by clay and all soil. However, a shift in the predominant frequency was observed only for the 'clay' type. The shift can be attributed to the fact that the 'clay' soil produces significant amplification even at longer periods (T = 0.5s – 1s) and few of the soil profiles under 'clay' site category have a natural period in the range of 0.8–1s causing resonance at the prolonged period. It is a common understanding that modeling taller soil column can modify the predominant period of spectral amplification. However [55], state that the amplification at the surface does not vary significantly for frequencies beyond the fundamental period of vibration (f_{sc}) of the soil column. It was observed that f_{sc} shifts towards lower resonant frequency as the intensity of the input motion increases and this explains the lower predominant frequency observed in Fig. 21. Hence, the generated surface spectrum is suitable for site-specific applications.

The seismic hazard map depicting the PGA values at the surface has been presented in Fig. 22. Majority of the study area are susceptible to moderate to high seismic hazard and the current codal provision underestimates the seismic as well as the amplification potential of the study area. As per IS 1893 [1], the study area belongs to zone III and susceptible to moderate ground shaking of PGA 0.16 g. The PGA values for design basis earthquake intensity level (10% probability of exceedance in 50 years) varies between 0.11 and 0.35 g. Hence, the findings highlight the necessity for site-specific studies in the Southern region of India whose seismic potential has been underestimated over the years.

7. Conclusions

The present study attempts to investigate the influence of local site amplification and incorporate the same for hazard computation in a probabilistic manner. In this regard, a number of borehole data were collected, processed and compiled in a systematic manner. The dynamic characteristics of the constituent layers in each bore log were modeled using suitable modulus reduction and damping curves. These modeled soil profiles were subjected to recorded ground motions selected and scaled to a target spectrum. The uniform hazard spectrum (UHS) for a reference site condition (V_s > 1500 ms^{-1}) was already available for the study region. The UHS was modified to generate target spectrum

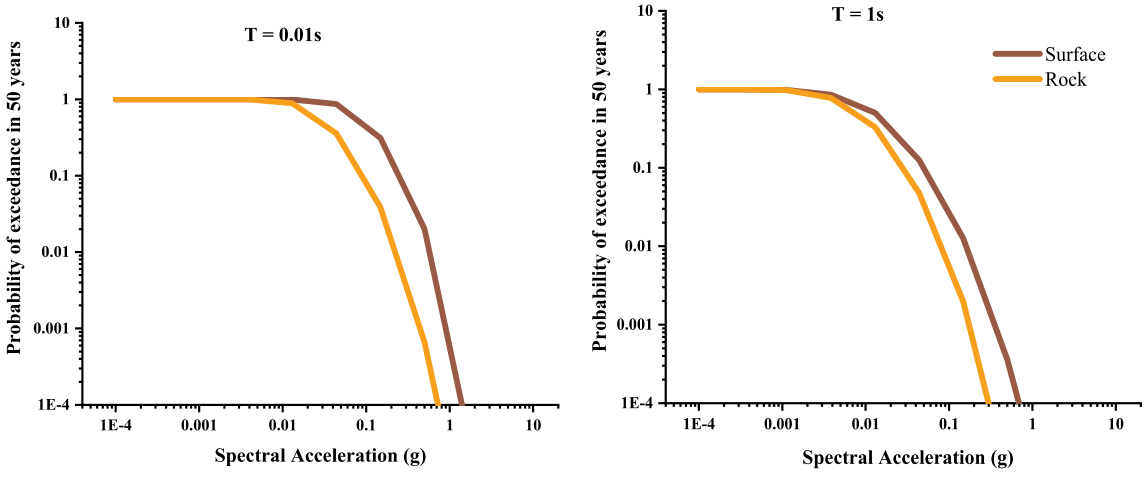

Fig. 20. Hazard curves for the rock and 'all soil' condition.

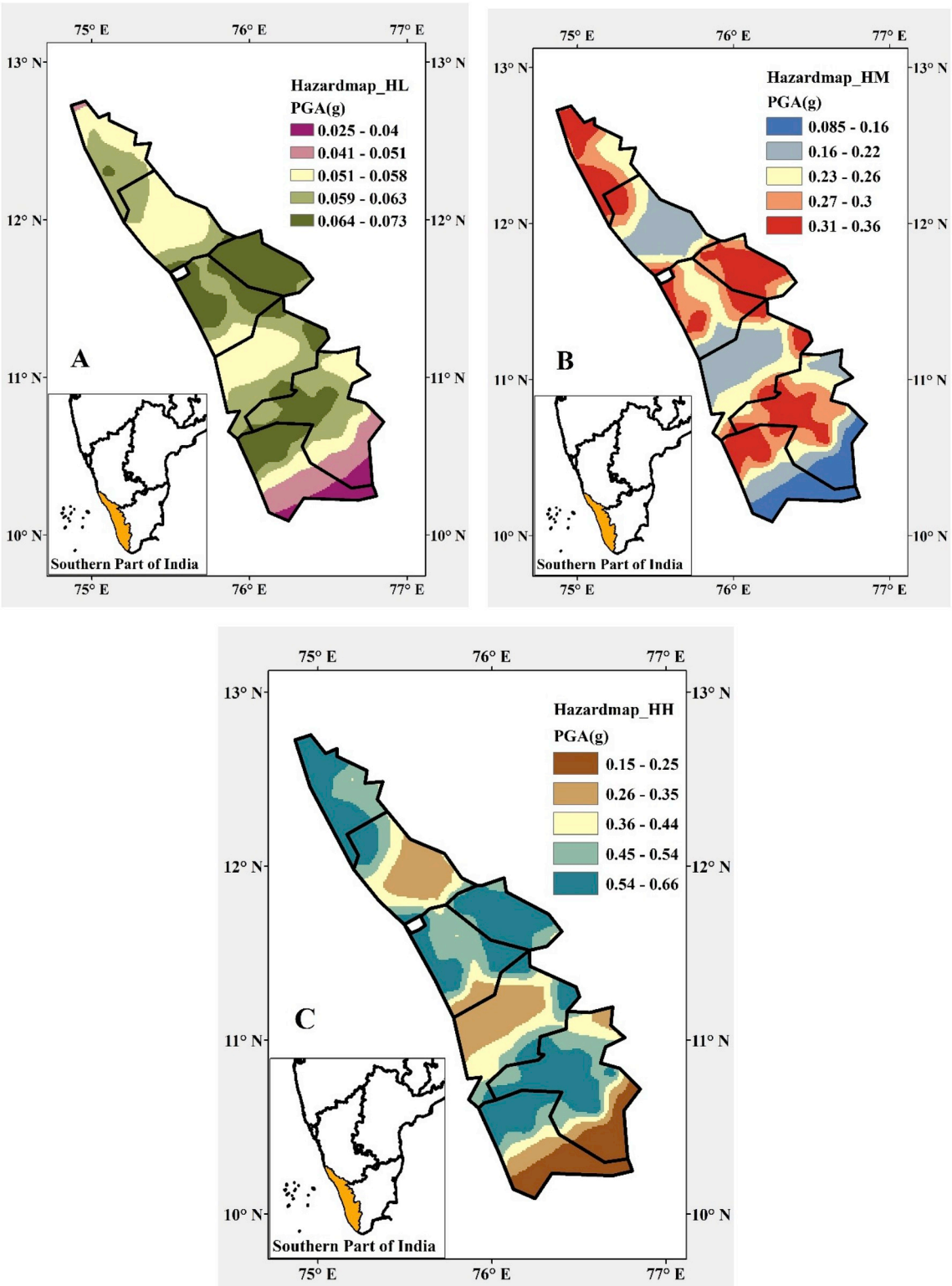

Fig. 22. Seismic hazard maps for the study region for **a.** 65% probability of exceedance, **b.** 10% probability of exceedance and **c.** 2.5% probability of exceedance in 50 years.

compatible with the local site condition. The target spectrum was developed for three hazard levels and the selected ground motion records were spectrally matched with the respective target spectrum. The nonlinear behavior of the soil to various input motions was captured using an equivalent linear approach. The computed amplification factors for various input motion intensity level (Spectral acceleration at 5% damping, S_a) was correlated using a nonlinear regression equation for various spectral periods. The amplification equations were developed for each soil type such as 'Clay', 'Sand' and 'all soil'. The site-specific PSHA was performed by transforming a generic GMPE into a site-specific one and integrating with the already developed seismic source model for the study area. Additionally, the local site effects were

studied by plotting incremental changes in the PGA value of the ground motion transmitted through each soil layer. The computed surface uniform hazard spectrum was compared with the elastic spectrum recommended by various seismic codes. The findings of the study are summarised below.

1. The soil profiles modeled in the study belongs to NEHRP 'C' (360-760 ms^{-1}) and 'D' (180–360 ms^{-1}) site categories and the study region belongs to seismic zone III (moderate level shaking).
2. The average spectral amplification observed is 3 for 'All soil' sites, 5 for 'clay' sites and 3.5 for 'sand' sites of the study region.
3. 'sand' sites exhibit nonlinear behavior by undergoing large amplification for smaller intensity measure but reduce substantially as the spectral acceleration values (S_a^r) values exceed 0.1 g. Among the three considered soil types, the 'sand' site is by far the highly nonlinear material and 'all soil' is less nonlinear.
4. 'clay' sites exhibit amplification even at longer periods (T = 0.8s, 1s, and 1.5s) but become less nonlinear with the increase in plasticity index. Hence, the 'clay' site plays a major role in the event of long-period seismic waves.
5. Three soil profiles of V_{S30} in the similar range demonstrated distinct amplification characteristics. The 'sand' site amplifies 33% (max. value) more than all soil and 29% more than the 'clay' site for lower S_a^r values. However, as the S_a^r (> 0.5 g) increases all soil amplifies 9% more than 'sand' soil. This observation implies that the local site amplification cannot be determined by $V_{s\ (30)}$ alone as the soil characteristics also influence the amplification.
6. The amplification characteristics observed in various spectral period frames suggests that PGA offers an unbiased and better prediction of amplification function. The same parameters studied at different spectral period suffers from resonance (site-specific effect) and demerits of the EQL method (computational capacity).
7. The comparison of the computed response spectra suggests that the seismic codes underestimate the spectral acceleration values for T < 0.25s and overestimates for T > 1s. The elastic response spectrum from NEHRP matches the estimated site-specific spectrum at the short period range.
8. The seismic hazard map suggests higher values of intensity measure (PGA) in the mid – Kerala region and the same extending towards South.

The procedure adopted in the investigation aims to reduce the uncertainty in various input parameters as well as the dilemma in adjusting a host response spectrum to target region. The overall amplification has been captured and integrated with the rock PSHA in the most robust way possible. The study provides a seismic hazard map at the surface level for the different probability of exceedance. These maps coupled with the site-specific spectrum can be used to plan, design and construct infrastructures of socio-economic importance. The outcome of the study can be further improved by accurate in-situ measurements of $V_{S\ (30)}$ and computing nonlinear site response in time domain. The research findings are region specific but the methodology adopted in the study can be repeated with reliable data for other regions as well.

Acknowledgment

The authors would like to thank Prof. S Chandrakaran, Mr. Mohanlal, Ms. Sreya M.V and staff of the Geotechnical division of NIT Calicut for their support and assistance in procuring the soil data. Dr. Arun P.R, scientist (CWRDM, Govt. of Kerala) shared the information related to bedrock depth for the study.

References

[1] Bureau of Indian Standard (BIS). IS 1893 - Indian standard criteria for earthquake resistant design of structures, Part 1 - general provisions and buildings. New Delhi, India: Bureau of Indian Standards; 2016.
[2] Atkinson GM, Boore DM. Earthquake ground-motion prediction equations for eastern North America. Bull Seismol Soc Am 2006;96(6):2181–205http://doi.org/10.1785/0120050245.
[3] Raghu Kanth STG, Iyengar RN. Estimation of seismic spectral acceleration in Peninsular India. J Earth Syst Sci 2007;116(3):199–214https://doi.org/10.1007/s12040-007-0020-8.
[4] Goulet CA, Eeri M, Stewart JP, Eeri M. Pitfalls of deterministic application of nonlinear site factors in probabilistic assessment of ground motions. Earthq Spectra 2009;25(3):541–55http://doi.org/10.1193/1.3159006.
[5] Bazzurro P, Cornell CA. Nonlinear soil-site effects in probabilistic seismic hazard analysis. Bull Seismol Soc Am 2004;94(6):2110–23.
[6] Ordonez Gustavo A. SHAKE2000 – a computer program for the 1-D analysis of geotechnical earthquake engineering problems. Lacey, Washington, USA: GeoMotions, LLC; 2012.
[7] Shreyasvi C, Venkataramana Katta, Chopra Sumer, Mohan Rout Madan. Probabilistic seismic hazard assessment of Mangalore and its adjoining regions, a part of Indian peninsular: an intraplate region. Pure and applied geophysics. Springer; 2019. https://doi.org/10.1007/s00024-019-02110-w.
[8] Soman K. Geology of Kerala. Bangalore - 560 019, India: Geological Society of India; 2002. P.B. No. 1922, Gavipuravzl R O.
[9] Valdiya KS. Neotectonic implication of collision of Indian and Asian plates 1980 Indian J Geol 1989;61:1–13.
[10] Rastogi BK, Chadha RK, Sarma CSP. Investigations of June 7, 1988 earthquake of magnitude 4.5 near Idukki Dam in southern India. In: Gupta HK, Chadha RK, editors. Induced seismicity. Pageoph topical volumes. Birkhäuser Basel; 1995. p. 109–22https://doi.org/10.1007/978-3-0348-9238-4_9.
[11] Nazimuddin M. "Coastal hydrology of Kozhikode, Kerala", doctoral dissertation. Kerala, India: Cochin University of Science and Technology; 2012http://hdl.handle.net/10603/3629.
[12] Joji VS. Ground water information booklet of Kozhikode district, Kerala state. " Central Ground Water Board, Ministry of Water Resources, Government of India; 2009.
[13] Balakrishnan P, Damodaran KT. "Hydrogeological and hydrochemical studies of the Periyar river basin, Central Kerala Doctoral dissertation Kerala, India: Cochin University Of Science And Technology; 2009
[14] Venkiteswaran CS, Rao BVLN. Report on the geophysical investigations for structural studies in the hard rock areas of mallapuram district, Kerala state (field). Pure Appl Chem 1980;52.
[15] Central Ground Water Board. "Mapping of hard rock aquifer system and aquifer management plan, Palakkad district, Kerala", draft report. 2002.
[16] Gopinath G. "An integrated hydrogeological study of the muvattupuzha river basin, Kerala, India.", doctoral dissertation. Kerala, India: Cochin University Of Science And Technology; 2003.
[17] Brijesh VK, V Diljith P, Ayisha VA. Geophysical resistivity surveys and well lithologs of filter point wells for aquifer delineation around Tavanur, Malappuram district, Kerala. National conference on recent trends in geoscience, material science and Civil engineering, Mysore, India, 23rd – 24th March 2017. 2017.
[18] Vinayachandran N, Joji VS. Ground water information booklet of Wayanad district, Kerala state. Central Ground Water Board; 2007.
[19] Sreenath G. Ground water information booklet of Kozhikode district, Kerala state. Central Ground Water Board, Ministry of Water Resources, Government of India; 2009.
[20] Saritha S, Vikas C. Ground water information booklet of Kannur district, Kerala state. Central Ground Water Board, Ministry of Water Resources, Government of India; 2009.
[21] IS2131. Method for standard penetration test for soils. New Delhi, India: Bureau of Indian Standard; 1981.
[22] Maheswari RU, Boominathan A, Dodagoudar GR. Use of surface waves in statistical correlations of shear wave velocity and penetration resistance of Chennai soils. Geotech Geol Eng 2010;28(2):119–37https://doi.org/10.1007/s10706-009-9285-9.
[23] Hanumantharao C, Ramana GV. Dynamic soil properties for microzonation of Delhi, India. J Earth Syst Sci 2008;117(2):719–30https://doi.org/10.1007/s12040-008-0066-2.
[24] Dikmen Ü. Statistical correlations of shear wave velocity and penetration resistance for soils. J Geophys Eng 2009;6(1):61–72https://doi.org/10.1088/1742-2132/6/1/007.
[25] Chatterjee K, Choudhury D. Variations in shear wave velocity and soil site class in Kolkata city using regression and sensitivity analysis. Nat Hazards 2013;69(3):2057–82https://doi.org/10.1007/s11069-013-0795-7.
[26] Kirar B, Maheshwari BK, Muley P. Correlation between shear wave velocity (vs) and SPT resistance (N) for Roorkee region. Int J Geosynth Gr Eng 2016;2:9https://doi.org/10.1007/s40891-016-0047-5.
[27] Hasancebi N, Ulusay R. Empirical correlations between shear wave velocity and penetration resistance for ground shaking assessments. Bull Eng Geol Environ 2007;66(2):203–13https://doi.org/10.1007/s10064-006-0063-0.
[28] Anbazhagan P, Kumar A, Sitharam TG. Seismic site classification and correlation between standard penetration test N value and shear wave velocity for Lucknow City in Indo-Gangetic Basin. Pure Appl Geophys 2013;170(3):299–318https://doi.org/10.1007/s00024-012-0525-1.
[29] Sil A, Haloi J. Empirical correlations with standard penetration test (SPT)-N for estimating shear wave velocity applicable to any region. Int J Geosynth Gr Eng 2017;3:22https://doi.org/10.1007/s40891-017-0099-1.
[30] Mhaske SY, Choudhury D. Geospatial contour mapping of shear wave velocity for Mumbai city. Nat Hazards 2011;59(1):317–27https://doi.org/10.1007/s11069-

011-9758-z.
[31] Thokchom S, Rastogi BK, Dogra NN, Pancholi V, Sairam B, Bhattacharya F, Patel V. Empirical correlation of SPT blow counts versus shear wave velocity for different types of soils in Dholera, Western India. Nat Hazards 2017;86(3):1291–306https://doi.org/10.1007/s11069-017-2744-3.
[32] Seed HB, Idriss IM. Soil moduli and damping factors for dynamic response analysis Berkeley, California: University of California; 1970. Report no. EERC 70-10.
[33] Sun JI, Golesorkhi R, Seed HB. Dynamic moduli and damping ratios of cohesive soils. Report No. UCB/EERC- 88/15. Berkeley, California: University of California; 1988.
[34] Gazetas G, Dakoulas P. Seismic analysis and design of rockfill dams: state-of-the-art. Soil Dynam Earthq Eng 1992;11(1):27–61https://doi.org/10.1016/0267-7261(92)90024-8.
[35] Vucetic M, Dobry R. Effect of soil plasticity on cyclic response. J Geotech Eng 1991;117(1):89–107https://doi.org/10.1061/(ASCE)0733-9410(1991)117:1(89).
[36] Seed HB, Sun JH. Implication of site effects in the Mexico city earthquake of september 19, 1985 for earthquake-resistance-design criteria in the San Francisco Bay area of California Berkeley, California: University of California; 1989. Report No. UCB/EERC-89/03.
[37] American Society of Civil Engineers. Minimum design loads and associated criteria for buildings and other structures, ASCE/SEI 7-16. 2017. Reston, vol. A https://doi.org/10.1061/9780784414248.
[38] Stewart JP, Afshari K. Guidelines for performing hazard-consistent one-dimensional ground response analysis for ground motion prediction. GEER reconnaissance of central Italy earthquake sequence View project Seismic soil liquefaction View project Retrieved from https://www.researchgate.net/publication/308052147 (DATE and TIME); 2015.
[39] Luzi L, Puglia R, Russo E, D'Amico M, Felicetta C, Pacor F, et al. "The engineering strong-motion database: a platform to access pan-European accelerometric data. Seismol Res Lett 2016;87(4):987–97https://doi.org/10.1785/0220150278.
[40] Rathje EM, Kottke AR, Trent WL. Influence of input motion and site property variabilities on seismic site response analysis. J Geotech Geoenviron Eng 2010;136(4)http://doi.org/10.1061/(ASCE)GT.1943-5606.0000255.
[41] Shreyasvi C, Badira Rahmath N, Venkataramana Katta. "Influence of variabilities in input parameters on seismic site response analysis", Lecture notes in Civil Engineering. Springer; 2019. (In press).
[42] Ansal A, Tönük G, Kurtuluş A. Implications of site-specific response analysis. Pitilakis K, editor. Recent advances in earthquake engineering in Europe. ECEE 2018. Geotechnical, geological and earthquake engineering, vol. 46. Cham: Springer; 2018. p. 51–68https://doi.org/10.1007/978-3-319-75741-4_2.
[43] Al-Atik L, Abrahamson NA. An improved method for nonstationary spectral matching. Earthq Spectra 2010;26(6):601–17https://doi.org/10.1193/1.3459159.
[44] ismosoft. SeismoMatch 2016 – a computer program for spectrum matching of earthquake records. 2016 available from http://www.seismosoft.com.
[45] Ktenidou OJ, Abrahamson NA. Empirical estimation of high-frequency ground motion on hard rock. Seismol Res Lett 2016;87(6):1465–78https://doi.org/10.1785/0220160075.
[46] Perron V, Hollender F, Bard P, Gélis C, Guyonnet-Benaize C, Hernandez B, Ktenidou O. Robustness of kappa (κ) measurement in low-to-moderate seismicity areas: insight from a site-specific study in provence, France. Bull Seismol Soc Am 2017;107(5):2272–92https://doi.org/10.1785/0120160374.
[47] Bard P, Bora SS, Hollender F, Laurendeau A, Traversa P, Bard P. Are the standard vs 30 -kappa host-to-target adjustments the best way to get consistent hard- rock ground motion prediction ? 2018. Best Practices in Physics-based Fault Rupture Models for Seismic Hazard Assessment of Nuclear Installations: issues and challenges towards full Seismic Risk Analysis , May 2018, Cadarache France. Best Practices in Physics-based Fault Rupture Models for Seismic Hazard Assessment of Nuclear Installations: issues and challenges towards full Seismic Risk Analysis, 2018 https://hal.archives-ouvertes.fr/hal-01826648.
[48] Laurendeau A, Cotton F, Ktenidou OJ, Bonilla LF, Hollender F. Rock and stiff-soil site amplification: dependency on VS30and Kappa (κ0). Bull Seismol Soc Am 2013;103(6):3131–48https://doi.org/10.1785/0120130020.
[49] Choi Y, Stewart JP. Nonlinear site amplification as function of 30 m shear wave velocity. Earthq Spectra 2005;21(1):1–30http://doi.org/10.1193/1.1856535.
[50] Kim B, Hashash YMA, Stewart JP, Rathje EM, Harmon JA, Musgrove MI, Silva WJ. Relative differences between nonlinear and equivalent-linear 1-D site response analyses. Earthquake spectra 2016http://doi.org/10.1193/051215EQS068M.
[51] Goulet CA, Stewart JP, Bazzurro P, Field EH. Integration of site-specific ground response analysis results into probabilistic seismic hazard analyses. Proceedings, 4th international conference on earthquake geotechnical engineering. 2007, June.
[52] Papaspiliou M, Kontoe S, Bommer JJ. An exploration of incorporating site response into PSHA-part II: sensitivity of hazard estimates to site response approaches. Soil Dynam Earthq Eng 2012;42:316–30https://doi.org/10.1016/j.soildyn.2012.05.001.
[53] BS EN1998-1. Eurocode 8: design of structures for earthquake resistance-part 1: general rules, seismic actions and rules for buildings. Brussels: European Committee for Standardization; 2005.
[54] ASCE. Seismic evaluation and retrofit of existing buildings. 2013.
[55] Bazzurro P, Cornell CA. Ground-motion amplification in nonlinear soil sites with uncertain properties. Bull Seismol Soc Am 2004;94(6):2090–109http://doi.org/10.1785/0120030215.